Cancer Science
The official journal of the Japanese Cancer Association

Cancer-associated missense mutations of caspase-8 activate nuclear factor-κB signaling

Mizuo Ando,[1,2] Masahito Kawazu,[1] Toshihide Ueno,[3] Kazutaka Fukumura,[1] Azusa Yamato,[3] Manabu Soda,[3] Yoshihiro Yamashita,[3] Young L. Choi,[1] Tatsuya Yamasoba[2] and Hiroyuki Mano[1,3,4,5,6]

Departments of [1]Medical Genomics; [2]Otolaryngology and Head and Neck Surgery, Graduate School of Medicine, University of Tokyo, Tokyo; [3]Division of Functional Genomics, Jichi Medical University, Tochigi; [4]Department of Cellular Signaling, Graduate School of Medicine, University of Tokyo, Tokyo; [5]CREST, Japan Science and Technology Agency, Saitama, Japan

(Received December 7, 2012/Revised April 26, 2013/Accepted May 6, 2013/Accepted manuscript online May 9, 2013/Article first published online June 7, 2013)

Head and neck squamous cell carcinoma (HNSCC) is an aggressive cancer with a 5-year survival rate of ~50%. With the use of a custom cDNA-capture system coupled with massively parallel sequencing, we have now investigated transforming mechanisms for this malignancy. The cDNAs of cancer-related genes (n = 906) were purified from a human HNSCC cell line (T3M-1 Cl-10) and subjected to high-throughput resequencing, and the clinical relevance of non-synonymous mutations thus identified was evaluated with luciferase-based reporter assays. A CASP8 (procaspase-8) cDNA with a novel G-to-C point mutation that results in the substitution of alanine for glycine at codon 325 was identified, and the mutant protein, CASP8 (G325A), was found to activate nuclear factor-κB (NF-κB) signaling to an extent far greater than that achieved with the wild-type protein. Moreover, forced expression of wild-type CASP8 suppressed the growth of T3M-1 Cl-10 cells without notable effects on apoptosis. We further found that most CASP8 mutations previously detected in various epithelial tumors also increase the ability of the protein to activate NF-κB signaling. Such NF-κB activation was shown to be mediated through the COOH-terminal region of the second death effector domain of CASP8. Although CASP8 mutations associated with cancer have been thought to promote tumorigenesis as a result of attenuation of the proapoptotic function of the protein, our results now show that most such mutations, including the novel G325A identified here, separately confer a gain of function with regard to activation of NF-κB signaling, indicating another role of CASP8 in the transformation of human malignancies including HNSCC. (*Cancer Sci* 2013; 104: 1002–1008)

Head and neck squamous cell carcinoma (HNSCC) is one of the most common types of human cancer, with an annual incidence of more than 500 000 cases worldwide.[1,2] The major risk factors for HNSCC are tobacco use, alcohol consumption, and infection with human papilloma virus.[3] It is an aggressive cancer with a propensity for local invasion and metastasis, which directly leads to disease- or treatment-related morbidity. The goals of HNSCC treatment are therefore not only to improve survival outcome but also to preserve vital physiological functions such as speech, breathing, swallowing, and hearing.

Most patients with HNSCC, however, present with advanced disease at the time of first evaluation and have a 5-year survival rate of only ~50%. Although advances in surgery and chemoradiation treatment have helped to preserve organ function in such individuals, they have resulted in only a moderate improvement in patient survival during the past 30 years. Characterization of the molecular mechanisms of HNSCC oncogenesis is expected to provide important information for the development of novel anticancer agents and the identification of biomarkers.

The recent advent of massively parallel sequencers, or next-generation sequencers, has rendered resequencing of the cancer genome manageable in private laboratories.[4] We have recently shown that a custom cDNA-capture system coupled with massively parallel sequencing provides a feasible and relatively simple approach for the simultaneous detection of point mutations, insertions/deletions (indels), and gene fusions among the captured genes.[5] Here we show that such high-throughput resequencing of targeted cDNAs from an oral squamous cell carcinoma cell line led to the identification of a missense mutation in caspase-8 (CASP8), a member of the cysteine–aspartic acid protease (caspase) family. Unexpectedly, CASP8 with this amino acid substitution (glycine-325 to alanine, or G325A) was found to activate signaling by the antiapoptotic transcription factor nuclear factor-κB (NF-κB) to an extent markedly greater than that observed with the wild-type protein. Of interest, most CASP8 mutants previously identified in human cancers were also found to activate the NF-κB pathway. As far as we are aware, a direct antiapoptotic effect of CASP8 in cancer has not previously been demonstrated.

Materials and Methods

Cell lines and plasmids. Human embryonic kidney 293T (HEK293T) cells, human oral squamous cell carcinoma T3M-1 Cl-10 cells, and human esophageal squamous cell carcinoma OE21 cells were obtained from RIKEN Cell Bank (Tsukuba, Japan), ATCC (Manassas, VA, USA), and European Collection of Cell Cultures (Salisbury, UK), respectively. All cells were maintained in DMEM–F12 supplemented with 10% FBS and 2 mM L-glutamine (all of which were from Invitrogen, Carlsbad, CA, USA). A full-length cDNA for the G325A mutant form of CASP8 was isolated by RT-PCR from T3M-1 Cl-10 cells and inserted into the retroviral plasmid pMXS.[6] Expression vectors for wild-type and previously identified mutant forms of CASP8 were generated by PCR-based mutagenesis. The nucleotide sequences of all constructs were confirmed by Sanger sequencing.

Resequencing coupled with a cDNA-capture system. Resequencing coupled with a custom cDNA-capture system was carried out as described previously.[5] In brief, RNA capture probes (Agilent Technologies, Santa Clara, CA, USA) designed to cover cDNAs of 906 human protein-coding genes were hybridized with cDNA fragments prepared from T3M-1 Cl-10 cells according to the protocols for the SureSelect Target Enrichment system (Agilent Technologies). Purified cDNA fragments were then subjected to deep sequencing for 76 bases from both ends with a Genome Analyzer IIx (GAIIx; Illumina, San Diego, CA, USA). Reads with a Q-value ≥20 at every

[6]To whom correspondence should be addressed.
E-mail: hmano@m.u-tokyo.ac.jp

doi: 10.1111/cas.12191

base were selected, and mapped to the reference cDNA sequences as well as the human genome sequence (GRCh37) with the Bowtie algorithm.[7] After removing single nucleotide polymorphisms (dbSNP build 32; http://www.ncbi.nlm.nih.gov/projects/SNP/snp_summary.cgi), non-synonymous mutations (≥30% mutation ratio at ≥30× coverage) for the target cDNAs were isolated by our in-house pipeline.

Luciferase-based reporter assays. The HEK293T cells were transfected with a CASP8 expression vector, the pGL-TK plasmid (Promega, Madison, WI, USA), and a luciferase-based reporter plasmid for signaling by c-Fos (pFL700),[8] c-Myc (pHXL),[9] β-catenin (TOP-flash; Upstate Biotechnology, Lake Placid, NY, USA), JNK (AP1; Panomics, Santa Clara, CA, USA), TP53,[10] Notch (pGa981-6),[11] Rho (pSRE.L),[12] MAPK (ELK1; Panomics), Gli (Genentech, South San Francisco, CA, USA), or NF-κB (Agilent Technologies). Luciferase activities were then assayed with a Dual-Luciferase Reporter Assay System (Promega), and the activity of firefly luciferase was normalized by that of *Renilla* luciferase.

Apoptosis and cell proliferation assays. The T3M-1 Cl-10 cells, which express CASP8(G325A), and OE21 cells, which express wild-type CASP8, were infected with a retrovirus generated from the pMXS-CASP8-ires-EGFP vector (Clontech, Mountain View, CA, USA), which allows simultaneous expression of CASP8 and enhanced green fluorescent protein (EGFP). The cells were then collected and assayed for apoptosis by staining with annexin V and propidium iodide (eBioscience, San Diego, CA, USA) followed by flow cytometry (FACSCanto II instrument; BD Biosciences, San Jose, CA, USA). Cell apoptosis was quantified by the Click-iT TUNEL Alexa Fluor Imaging Assay (Invitrogen). Cell proliferation was assayed by flow cytometric determination of the cell fraction positive for EGFP.

Statistical analysis. Quantitative data are presented as means ± SD and were compared with Student's *t*-test. A *P*-value of <0.05 was considered statistically significant.

Results

Identification of a CASP8 mutation in T3M-1 Cl-10 cells. To identify oncogenes for oral squamous cell carcinoma, we selected cDNA fragments for cancer-related genes (n = 906) from T3M-1 Cl-10 oral squamous cell carcinoma cells with the use of our custom cDNA-capture system.[5] Deep sequencing of such fragments with a GAIIx sequencer yielded 91 961 299 independent high-quality reads that mapped to 850 cDNAs with a mean coverage of 1202 reads/bp. Screening for missense mutations, indels, and gene fusions with our in-house computational pipeline resulted in the identification of 12 non-synonymous mutations that were further confirmed by Sanger sequencing (Table 1). We did not detect any indels or gene fusions that were confirmed by the capillary sequencing.

The 12 missense mutations include a novel G-to-C change at position 1183 of *CASP8* cDNA (GenBank accession number, NM_033355.3), which results in a glycine-to-alanine substitution at codon 325 of the encoded protein (Fig. 1a), as well as known HNSCC-related mutations such as those in *TP53* and *HRAS*. In our deep sequencing data, this substituted position of *CASP8* cDNA was read at a depth of ×469 and showed a mutation ratio of 98.5%, indicative of loss of heterozygosity at this locus.

The *CASP8* gene encodes the inactive (pro) form of CASP8, which plays an essential role in the execution of apoptosis.[13] Caspase-8 is composed of a COOH-terminal catalytic domain and an NH_2-terminal prodomain region that contains two tandem death effector domains (DEDs) (Fig. S1). Activation of CASP8 requires autoproteolysis that generates a heterodimer consisting of large (p20) and small (p10) protease subunits. The G325A mutation of CASP8 is located near the catalytic site in the p20 subunit.

Mutant CASP8(G325A) activates the NF-κB signaling pathway. To evaluate the biological relevance of the CASP8 (G325A) mutant, we carried out a reporter assay for a wide range of intracellular signaling pathways. Wild-type CASP8 markedly increased reporter activity for the NF-κB pathway (Fig. 1b), consistent with previous observations.[14,15] The G325A mutant of CASP8, however, increased such reporter activity to an extent far greater than that observed with the wild-type protein. In contrast, the effects of the wild-type and mutant forms of CASP8 on other signaling pathways, including those mediated by c-Fos, c-Myc, β-catenin, JNK, TP53, Notch, Rho, MAPK, and Gli, did not differ significantly (Fig. 1c), indicating that the G325A mutation influences NF-κB signaling specifically.

Catalytic activity of CASP8 and its mutants was also examined. The wild-type CASP8, CASP8(G325A), CASP8(C360A) (an amino acid substitution at the catalytic center),[16] CASP8 (D210A/D216A) (double mutations at the autoprocessing region), or CASP8(D210A/D216A/D223A) (triple mutations at the autoprocessing region), was introduced into HEK293 cells that were then subjected to an enzymatic assay for CASP8. As expected, wild-type CASP8 is catalytically active in HEK293, but a mutation at its catalytic center almost abolished its processing potency (Fig. 2a). Interestingly, the G325A substitution severely hampered CASP8 activity. In contrast, CASP8 with mutations at the autoprocessing region carry a decreased, but apparent, processing ability.

To examine whether the G350A mutation contributes directly to malignant transformation, we infected T3M-1 Cl-10 cells harboring the mutant *CASP8* gene with a retrovirus encoding both EGFP and either wild-type CASP8 or the

Table 1. Non-synonymous mutations detected in T3M-1 Cl-10 cells

Gene	GenBank accession no.	Read coverage	Mismatch reads (%)	Nucleotide change	Amino acid change
CASP8	NM_033355	×469	98.5	1183G>C	G325A
ELF4	NM_001421	×188	39.8	1016C>A	L211M
GSG2	NM_031965	×119	100.0	1238T>C	V402A
HRAS	NM_005343	×613	25.1	370A>T	Q61L
IRAK2	NM_001570	×155	49.0	591C>T	S172L
NUAK2	NM_030952	×162	51.2	1427G>A	A434T
PDPK1	NM_002613	×226	37.6	1663G>C	E507Q
PRKCZ	NM_002744	×61	49.1	306C>T	R49C
PXK	NM_017771	×82	57.3	364A>G	I89V
RHOA	NM_001664	×1127	52.9	394G>C	E40Q
TP53	NM_000546	×234	97.8	1035A>G	R280G
TTBK2	NM_173500	×100	51.0	1402G>C	L321F

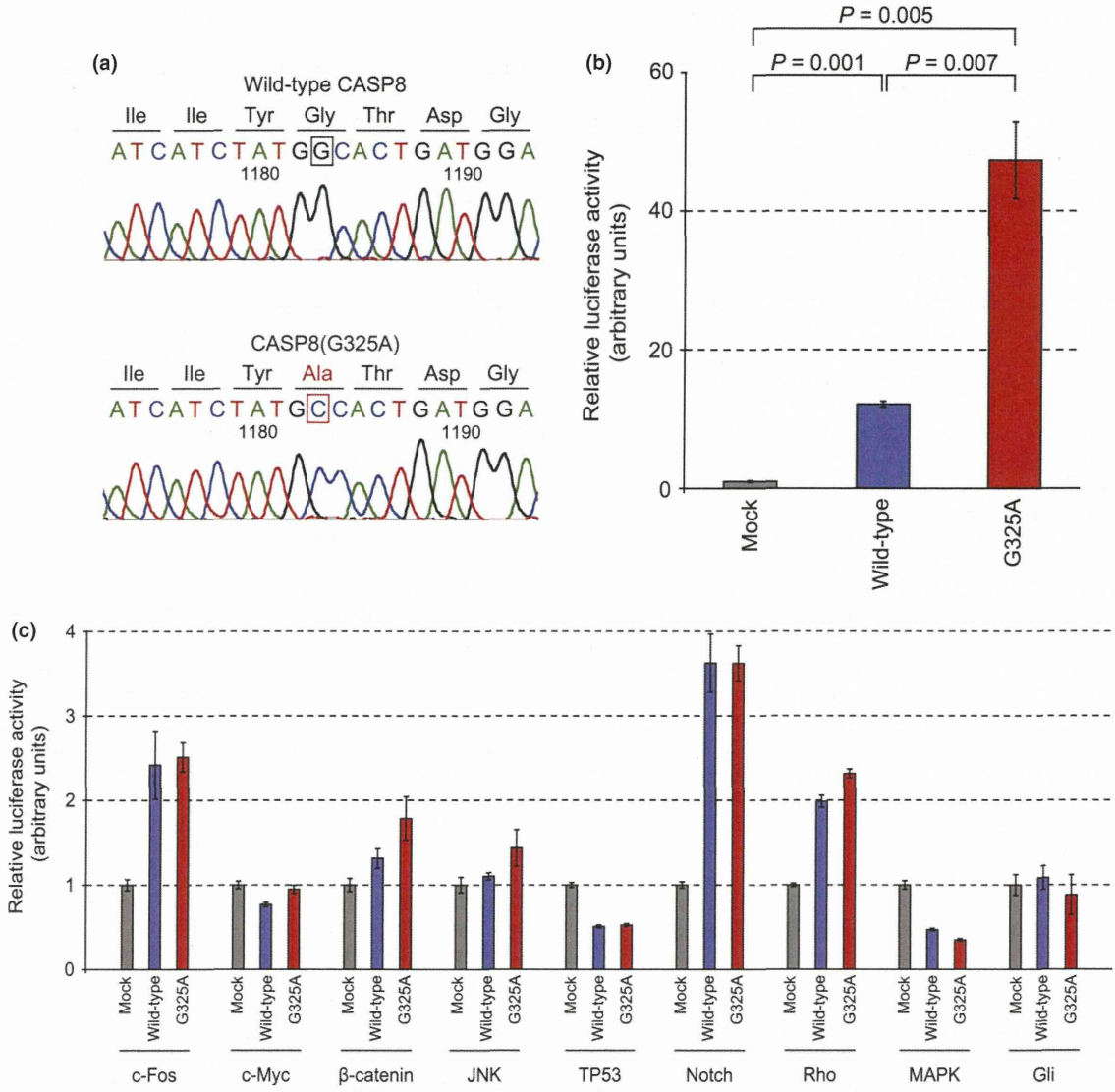

Fig. 1. Mutant protein CASP8(G325A) selectively activates the nuclear factor-κB (NF-κB) signaling pathway. (a) Electrophoretograms of *CASP8* cDNA identified an 1183G > C substitution, which results in a G325A amino acid substitution, in T3M-1 Cl-10 cells. (b,c) HEK293T cells were transfected with an expression vector for CASP8 or CASP8(G325A) or with the corresponding empty vector (Mock) together with pGL-TK and reporter plasmids for NF-κB (b) or other (c) signaling pathways, after which the cells were lysed and assayed for luciferase activities. The activity of firefly luciferase was normalized by that of *Renilla* luciferase then expressed relative to the corresponding value for mock-transfected cells. Data are means ± SD from three independent experiments. *P*-values were calculated using Student's *t*-test.

G325A mutant, then assayed the proliferation of EGFP-positive cells. Surprisingly, forced expression of wild-type CASP8 resulted in a marked reduction in the number of EGFP-positive cells, whereas the G325A mutant had only a slight effect on cell number (Fig. 2b). This suppression of cell growth by wild-type CASP8 was not observed in another squamous cell carcinoma cell line, OE21, which harbors the wild-type *CASP8* gene (Fig. 2b).

Interestingly, while annexin V-positive fraction was marginally increased in T3M-1 Cl-10 cells overexpressing wild-type CASP8 (Fig. S2), neither CASP8 nor CASP8 (G325A) induced notable apoptosis in T3M-1 Cl-10, as judged by the TUNEL assay (Fig. 2c). It is, therefore, possible that CASP8 regulation of cell growth in cancer may be independent, in part, of its apoptosis-inducing function.

We further depleted the *CASP8* message in T3M-1 Cl-10 by the use of siRNA, and examined its effects on the expression of NF-κB targets. As shown in Figure S3, decrease in the *CASP8* message led to a marked suppression in *BCL2* expression, supporting the positive role of CAPS8 in NF-κB signaling.

CASP8 mutations in human tumors. Non-synonymous mutations in CASP8 have been previously reported in various epithelial tumor types including gastric cancer (GC), colorectal cancer, hepatocellular carcinoma, and HNSCC.[16–19] These mutations include seven missense, one nonsense, and six frameshift mutations as well as one in-frame deletion (Fig. S1, Table S1). Whereas such mutations have been thought to contribute to carcinogenesis through a loss of the proapoptotic function of CASP8, we unexpectedly found that most of the mutants markedly activated NF-κB signaling (Fig. 3), suggestive of a gain of function with regard to such signaling. Of note, all of the three CASP8 mutants (GC1, GC4, and GC7) that failed to activate NF-κB signaling harbor non-synonymous mutations within the DEDs, suggesting that these domains may be essential for NF-κB activation.

In addition, screening as of January 2013 for non-synonymous mutations in CASP8 among public databases for

doi: 10.1111/cas.12191

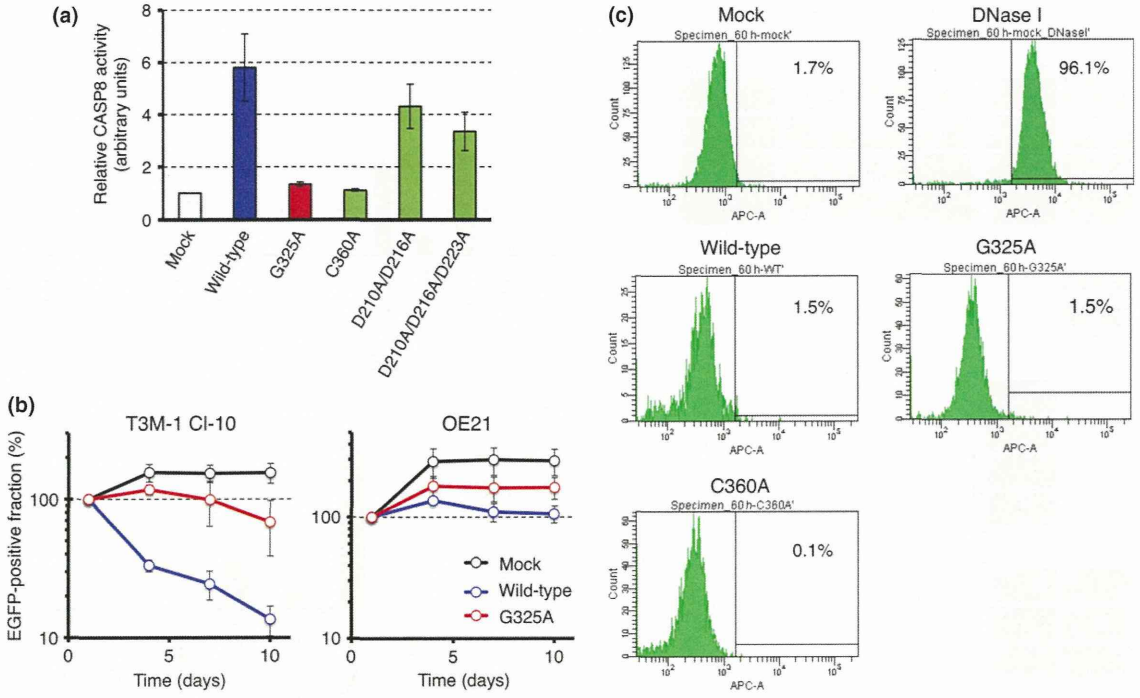

Fig. 2. Caspase-8 (CASP8) suppresses the proliferation of T3M-1 Cl-10 cells but not that of OE21 cells. (a) Proteolytic activity of CASP8 was measured with the Caspase-Glo8 assay for HEK293 cells expressing wild-type CASP8, CASP8(G325A), CASP8(C360A), CASP8(D210A/D216A), or CASP8(D210A/D216A/D223A), and is shown relative to the value for mock-transfected cells. Data are means ± SD from three independent experiments. (b) T3M-1 Cl-10 cells (left panel) or OE21 cells (right panel) were infected with a retrovirus encoding enhanced green fluorescent protein (EGFP) either alone (Mock) or together with wild-type or G325A mutant forms of CASP8. The number of EGFP-positive cells was then measured by flow cytometry at 1, 4, 7, and 10 days after infection and is expressed as a percentage of that at 1 day after infection. Data are means ± SD from three independent experiments. (c) Fragmented DNA in apoptotic cells was quantified by TUNEL assay for T3M-1 Cl-10 cells infected with an empty virus (Mock), or virus expressing wild-type, G325A mutant, or C360A mutant of CASP8. Fractions of cells with fragmented DNA are indicated as percentages. T3M-1 Cl-10 cells treated with DNase I were used as a positive control of apoptosis.

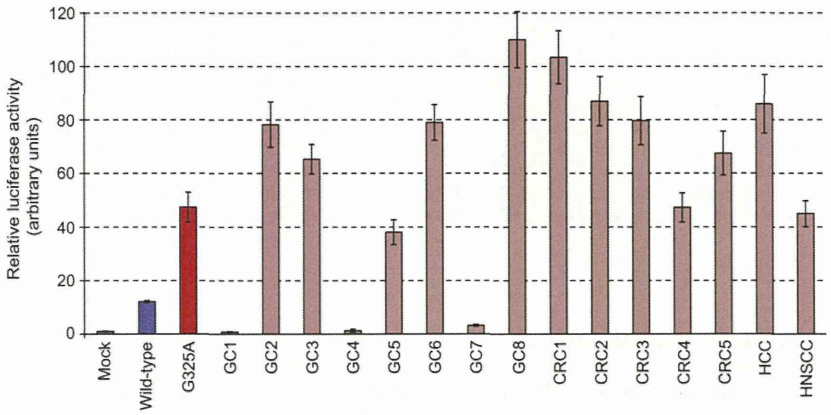

Fig. 3. Tumor-associated caspase-8 (CASP8) mutants activate the nuclear factor-κB pathway. HEK293T cells were transfected with a luciferase reporter plasmid for nuclear factor-κB, with pGL-TK, and with expression vectors for wild-type or the indicated mutant forms of CASP8. Normalized firefly luciferase activity was then determined and expressed relative to the value for mock-transfected cells. Data are means ± SD from three independent experiments. CRC, colorectal cancer; GC, gastric cancer; HCC, hepatocellular carcinoma; HNSCC, head and neck squamous cell carcinoma.

cancer genome mutations (COSMIC version 62, http://cancer.sanger.ac.uk/cancergenome/projects/cosmic/; The Cancer Genome Atlas, https://tcga-data.nci.nih.gov/tcga/tcgaHome2.jsp; and the International Cancer Genome Consortium, http://icgc.org) list 76 independent missense/nonsense mutations, seven frame-shift indels within CASP8, many of which had been confirmed to be somatic changes. Interestingly, amino acid substitutions at Gly-325 (including G325A) were identified in multiple cancer specimens (such as those for large intestine carcinoma and cervical squamous cell carcinoma), suggesting that missense mutations at this position are recurrent.

Caspase-8 domains linked to NF-κB activation. To investigate further how CASP8 controls the NF-κB pathway, we generated a series of CASP8 mutants (Fig. 4a). As shown in Figure 4(b), the D210A/D216A mutant is still able to activate NF-κB signaling by an extent similar to that achieved with the wild-type protein. Similarly, the addition of both D210A and D216A

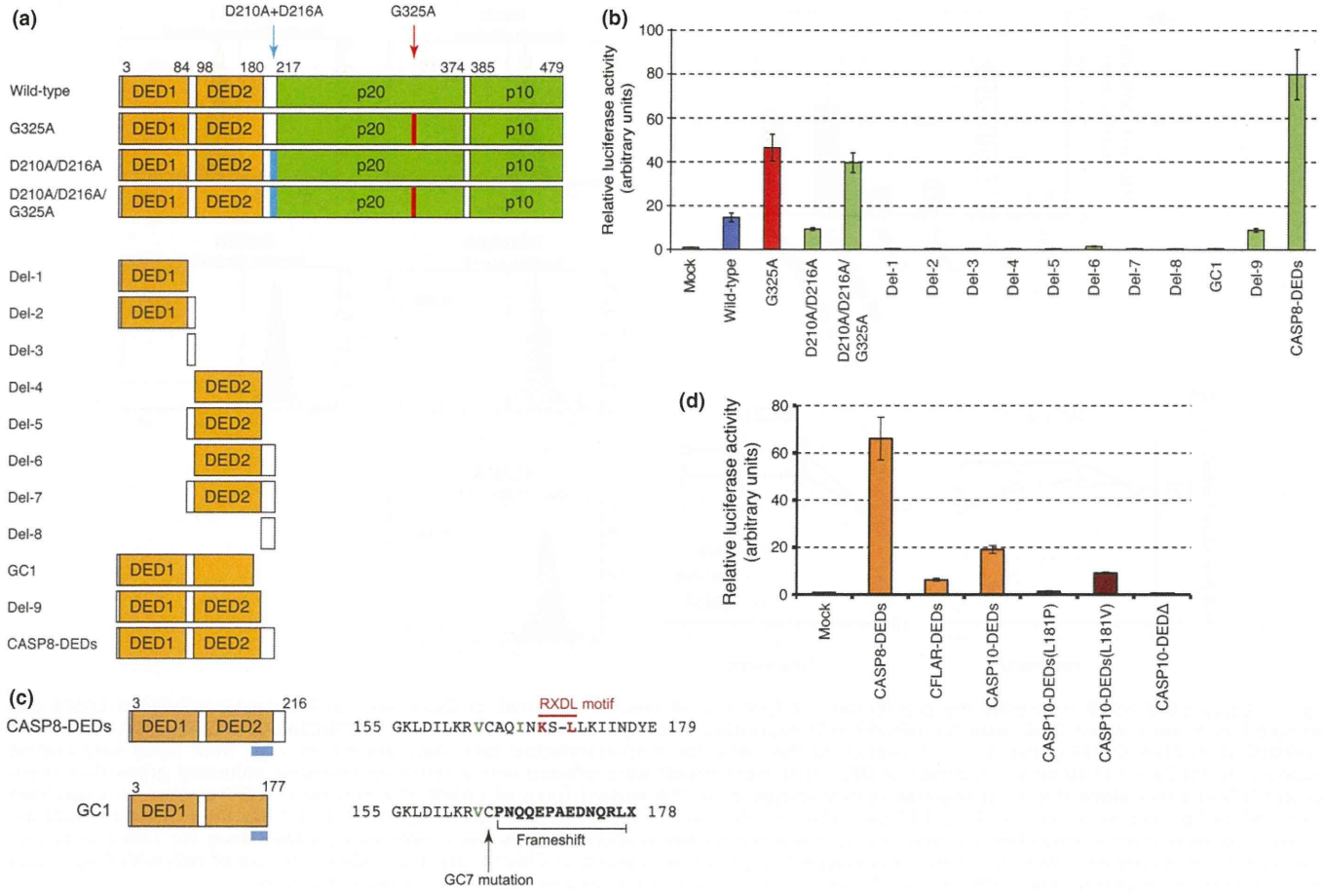

Fig. 4. Death effector domains (DEDs) activate nuclear factor-κB (NF-κB) signaling. (a) The protein structure of caspase-8 (CASP8) mutants is shown schematically with amino acid numbers indicated at the top. In addition to the wild-type and D210A/D216A mutant forms with or without the G325A substitution, various constructs for the DED and Hinge regions (Del-1 to Del-9) were generated. The structure of the mutant from cancer specimen GC1 and a mutant encompassing both DEDs and Hinge regions (CASP8-DEDs) is also shown. (b) Expression plasmids for the CASP8 mutants in (A) were introduced into HEK293T cells for the NF-κB reporter assay. Normalized firefly luciferase activity is expressed relative to the value for mock-transfected cells. Data are means ± SD from three independent experiments. (c) Amino acid sequences of the COOH-terminal regions (depicted by light blue bars in the left panel) of CASP8-DEDs and the CASP8 mutant from specimen GC1 are shown at the right. The conserved RXDL motif is indicated in red, and Val^{163} and Ile^{167} residues that contribute to the conserved hydrophobic patch are indicated in green. In the GC1 mutant, a frameshift deletion changes the amino acid sequence after Cys^{164} and generates a termination codon. The GC7 mutant has a C164Y substitution that markedly attenuates CASP8-induced NF-κB activation. (d) The ability to activate the NF-κB pathway was examined for CASP8-DEDs and the corresponding regions of CFLAR (amino acid residues 1–196) and CASP10 (residues 1–219), as in (b). For CASP10, we also examined the DED region with a L181P or L181V substitution, or RXDL-deleted DEDΔ encompassing only amino acid residues 1–175.

substitutions to CASP8(G325A) did not substantially affect its ability to activate the NF-κB pathway.

We also generated expression constructs for the NH_2-terminal DED (DED1) or COOH-terminal DED (DED2) either alone or together with the Hinge regions between DED1 and DED2 (Hinge-1) or between DED2 and p20 (Hinge-2) (Fig. 4a). None of these deletion mutants activated the NF-κB pathway (Fig. 4b). In contrast, a deletion mutant consisting of the entire prodomain (CASP8-DEDs) activated NF-κB signaling to a level even higher than that induced by CASP8 (G325A). Deletion of Hinge-2 from CASP8-DEDs (the Del-9 mutant) markedly reduced the stimulatory effect on NF-κB signaling. A *CASP8* cDNA previously identified in the specimen designated GC1 has a 2-bp deletion (Table S1) that results in premature termination within DED2 (Fig. 4c). This truncation almost completely abrogated the ability of CASP8 to activate NF-κB signaling (Figs 3,4b). Both Hinge-2 and the COOH-terminal end of DED2 thus likely play an essential role in the regulation of NF-κB signaling by CASP8. This notion was reinforced by the observation that a Cys^{164}-to-Tyr substitution at the COOH-terminal end of DED2 previously identified in the GC7 specimen (Table S1, Fig. 4c) also largely abolished the ability of CASP8 to activate NF-κB signaling (Fig. 3).

Members of the DED family of proteins possess a key hydrophobic patch (for DED–DED interactions) that is exposed at the surface of each molecule and includes the conserved RXDL motif (corresponding to "KS – L" in DED2 of CASP8) in the COOH-terminal region of the DED.[20–22] Our findings are thus consistent with the idea that this conserved region contributes to the regulation of NF-κB.

Prodomains of CASP8-related proteins are able to activate NF-κB signaling. Given that the prodomain of CASP8 is sufficient to fully active NF-κB signaling, we tested whether the prodomains of the CASP8-related proteins CFLAR (also known as cFLIPL) and caspase-10 (CASP10) might have similar effects. CFLAR is structurally similar to CASP8 but does not possess functional caspase activity, given that it does not

doi: 10.1111/cas.12191

contain the conserved catalytic cysteine residue found in all functional caspases.[23] Caspase-10 is highly homologous to CASP8 and is also recruited to, and becomes activated by, death receptors.[24–26] We found that the entire prodomains of CFLAR and CASP10 each markedly increased the level of NF-κB signaling (Fig. 4d) as already shown for CASP10 by other groups.[27] Although conservation of the RXDL motif is less clear in CASP10 compared to the other members (Fig. S4), substitution of the conserved Leu^{181} in CASP10 to either Pro or Val residues attenuated its NF-κB-activating potential (Fig. 4d). Furthermore, the CASP10-DEDs protein lacking the putative RXDL region completely lost such ability, confirming the essential role of the DEDs COOH-terminus in CASP10 activation of the NF-κB pathway.

Discussion

One of the most proximal caspases in the apoptosis cascade, CASP8 is driven by the death-inducing signaling complex in response to ligation of death receptors[13] such as tumor necrosis factor receptor 1, CD95 (Fas, or Apo1), and tumor necrosis factor-related apoptosis-inducing ligand (TRAIL, or Apo2L) receptor. Activation of CASP8 requires dimerization and consequent autocleavage of the procaspase-8 zymogen,[28] and it initiates the extrinsic apoptosis cascade through activation of downstream effectors such as CASP3, CASP6, and CASP7.[29]

In addition, CASP8 has the potential to activate the antiapoptotic transcription factor NF-κB through its tandem DED region,[14,15,30] and IκB kinase γ (IKKγ), an essential regulatory subunit of the IKK complex, participates in this CASP8-mediated activation of NF-κB.[31] The tandem DEDs of CFLAR also directly interact with and recruit IKKγ and thereby activate NF-κB.[32] However, we failed to detect a direct association between the tandem DEDs of CASP8 and IKKγ (data not shown). How the tandem DEDs of CASP8 mediate NF-κB activation thus remains unclear. Given the essential role of the COOH-terminal region of DED2 and the Hinge-2 region of CASP8 in the activation of NF-κB, it will be of interest to profile the cellular proteins that associate with these regions. Importantly, whereas somatic non-synonymous mutations in *CASP8* are detected relatively frequently in human tumors, the mutant proteins have been assumed to accelerate carcinogenesis as a result of a loss of proapoptotic function.[16,18,19]

In contrast, our data now suggest that many of the somatic mutations within *CASP8* in human cancer provide simultaneously inactivation of its proapoptotic function and activation of NF-κB signaling. Additionally, restoration of *CASP8* expression in a *CASP8*-mutant cell line (T3M-1 Cl-10) clearly suppressed cell proliferation without apparent effects on apoptosis, further confirming the relevance of *CASP8* mutation on carcinogenesis. It should be noted, however, that our data does not prove a direct linkage between an enhanced NF-κB signaling and cell growth. It may be possible that CASP8 mutants exert cancer-promoting functions other than the activation of NF-κB pathway.

Importantly, a recent large-scale exome sequencing of HNSCC specimens ($n = 74$) detected somatic mutations of *CASP8* in 8% of tumors,[33] suggestive of an unexpected and transforming role of CASP8 in HNSCC (and maybe also in other epithelial tumors). Whereas activation of NF-κB is frequently detected in a wide array of human malignancies, little is known about the exact mechanisms underlying such activation. Our results show that somatic mutation of *CASP8* may be one such mechanism, and they suggest the possibility of treating *CASP8* mutation-positive tumors with inhibitors of NF-κB, or targeting other proteins that contribute to the NF-κB activation pathway.

Acknowledgments

This study was supported in part by a grant for Research on Human Genome Tailor-made from the Ministry of Health, Labor, and Welfare of Japan, by Grants-in-Aid for Scientific Research (B) from the Japan Society for the Promotion of Science, from The Yasuda Medical Foundation, from The Sagawa Foundation for Promotion of Cancer Research, and from The Mitsubishi Foundation.

Disclosure Statement

The authors have no conflict of interest.

References

1 Mao L, Hong WK, Papadimitrakopoulou VA. Focus on head and neck cancer. *Cancer Cell* 2004; **5**: 311–6.
2 Haddad RI, Shin DM. Recent advances in head and neck cancer. *N Engl J Med* 2008; **359**: 1143–54.
3 Argiris A, Karamouzis MV, Raben D, Ferris RL. Head and neck cancer. *Lancet* 2008; **371**: 1695–709.
4 Mardis ER. A decade's perspective on DNA sequencing technology. *Nature* 2011; **470**: 198–203.
5 Ueno T, Yamashita Y, Soda M *et al.* High-throughput resequencing of target-captured cDNA in cancer cells. *Cancer Sci* 2012; **103**: 131–5.
6 Onishi M, Kinoshita S, Morikawa Y *et al.* Applications of retrovirus-mediated expression cloning. *Exp Hematol* 1996; **24**: 324–9.
7 Langmead B, Trapnell C, Pop M, Salzberg SL. Ultrafast and memory-efficient alignment of short DNA sequences to the human genome. *Genome Biol* 2009; **10**: R25.
8 Hu Q, Milfay D, Williams LT. Binding of NCK to SOS and activation of ras-dependent gene expression. *Mol Cell Biol* 1995; **15**: 1169–74.
9 Takeshita T, Arita T, Higuchi M *et al.* STAM, signal transducing adaptor molecule, is associated with Janus kinase and involved in signaling for cell growth and c-myc induction. *Immunity* 1997; **6**: 449–57.
10 El-Deiry WS, Tokino T, Velculescu VE *et al.* WAF1, a potential mediator of p53 tumor suppression. *Cell* 1993; **75**: 817–25.
11 Kurooka H, Kuroda K, Honjo T. Roles of the ankyrin repeats and C-terminal region of the mouse notch1 intracellular region. *Nucleic Acids Res* 1998; **26**: 5448–55.
12 Hill CS, Wynne J, Treisman R. The Rho family GTPases RhoA, Rac1, and CDC42Hs regulate transcriptional activation by SRF. *Cell* 1995; **81**: 1159–70.
13 Muzio M, Chinnaiyan AM, Kischkel FC *et al.* FLICE, a novel FADD-homologous ICE/CED-3-like protease, is recruited to the CD95 (Fas/APO-1) death–inducing signaling complex. *Cell* 1996; **85**: 817–27.
14 Chaudhary PM, Eby MT, Jasmin A, Kumar A, Liu L, Hood L. Activation of the NF-kappaB pathway by caspase 8 and its homologs. *Oncogene* 2000; **19**: 4451–60.
15 Hu WH, Johnson H, Shu HB. Activation of NF-kappaB by FADD, Casper, and caspase-8. *J Biol Chem* 2000; **275**: 10838–44.
16 Soung YH, Lee JW, Kim SY *et al.* Caspase-8 gene is frequently inactivated by the frameshift somatic mutation 1225_1226delTG in hepatocellular carcinomas. *Oncogene* 2005; **24**: 141–7.
17 Mandruzzato S, Brasseur F, Andry G, Boon T, van der Bruggen P. A CASP-8 mutation recognized by cytolytic T lymphocytes on a human head and neck carcinoma. *J Exp Med* 1997; **186**: 785–93.
18 Kim HS, Lee JW, Soung YH *et al.* Inactivating mutations of caspase-8 gene in colorectal carcinomas. *Gastroenterology* 2003; **125**: 708–15.
19 Soung YH, Lee JW, Kim SY *et al.* CASPASE-8 gene is inactivated by somatic mutations in gastric carcinomas. *Cancer Res* 2005; **65**: 815–21.
20 Eberstadt M, Huang B, Chen Z *et al.* NMR structure and mutagenesis of the FADD (Mort1) death-effector domain. *Nature* 1998; **392**: 941–5.
21 Tibbetts MD, Zheng L, Lenardo MJ. The death effector domain protein family: regulators of cellular homeostasis. *Nat Immunol* 2003; **4**: 404–9.
22 Yu JW, Shi Y. FLIP and the death effector domain family. *Oncogene* 2008; **27**: 6216–27.

23 Budd RC, Yeh WC, Tschopp J. cFLIP regulation of lymphocyte activation and development. *Nat Rev Immunol* 2006; **6**: 196–204.
24 Kischkel FC, Lawrence DA, Tinel A *et al.* Death receptor recruitment of endogenous caspase-10 and apoptosis initiation in the absence of caspase-8. *J Biol Chem* 2001; **276**: 46639–46.
25 Wang J, Chun HJ, Wong W, Spencer DM, Lenardo MJ. Caspase-10 is an initiator caspase in death receptor signaling. *Proc Natl Acad Sci USA* 2001; **98**: 13884–8.
26 Sprick MR, Rieser E, Stahl H, Grosse-Wilde A, Weigand MA, Walczak H. Caspase-10 is recruited to and activated at the native TRAIL and CD95 death-inducing signalling complexes in a FADD-dependent manner but can not functionally substitute caspase-8. *EMBO J* 2002; **21**: 4520–30.
27 Shikama Y, Yamada M, Miyashita T. Caspase-8 and caspase-10 activate NF-kappaB through RIP, NIK and IKKalpha kinases. *Eur J Immunol* 2003; **33**: 1998–2006.
28 Pop C, Fitzgerald P, Green DR, Salvesen GS. Role of proteolysis in caspase-8 activation and stabilization. *Biochemistry* 2007; **46**: 4398–407.
29 Krammer PH. CD95's deadly mission in the immune system. *Nature* 2000; **407**: 789–95.
30 Heyninck K, Beyaert R. Crosstalk between NF-kappaB-activating and apoptosis-inducing proteins of the TNF-receptor complex. *Mol Cell Biol Res Commun* 2001; **4**: 259–65.
31 Varfolomeev E, Maecker H, Sharp D *et al.* Molecular determinants of kinase pathway activation by Apo2 ligand/tumor necrosis factor-related apoptosis-inducing ligand. *J Biol Chem* 2005; **280**: 40599–608.
32 Golks A, Brenner D, Krammer PH, Lavrik IN. The c-FLIP-NH2 terminus (p22-FLIP) induces NF-kappaB activation. *J Exp Med* 2006; **203**: 1295–305.
33 Stransky N, Egloff AM, Tward AD *et al.* The mutational landscape of head and neck squamous cell carcinoma. *Science* 2011; **333**: 1157–60.

Supporting Information

Additional Supporting Information may be found in the online version of this article:

Fig. S1. Non-synonymous mutations in caspase-8. CRC, colorectal cancer; GC, gastric cancer; HCC, hepatocellular carcinoma; HNSCC, head and neck squamous cell carcinoma.

Fig. S2. Caspase-8 (CASP8) affects annexin V-positive fractions in T3M-1 Cl-10 head and neck squamous cell carcinoma cells but not in OE21 esophageal squamous cell carcinoma cells.

Fig. S3. Depletion of *CASP8* message leads to a decrease in *BCL2* expression.

Fig. S4. Structure of human death effector domain (DED) family members.

Table S1. Caspase-8 (CASP8) non-synonymous mutations identified in previously published reports.

doi: 10.1111/cas.12191

Miyanaga et al. BMC Cancer 2013, 13:262
http://www.biomedcentral.com/1471-2407/13/262

BMC Cancer

CASE REPORT Open Access

Activity of EGFR-tyrosine kinase and ALK inhibitors for *EML4–ALK*-rearranged non–small–cell lung cancer harbored coexisting *EGFR* mutation

Akihiko Miyanaga[1], Kumi Shimizu[1], Rintaro Noro[1], Masahiro Seike[1], Kazuhiro Kitamura[1], Seiji Kosaihira[1], Yuji Minegishi[1], Takehito Shukuya[7], Akinobu Yoshimura[1,8], Masashi Kawamoto[2,3], Shinichi Tsuchiya[2], Koichi Hagiwara[4], Manabu Soda[5], Kengo Takeuchi[6], Nobuyuki Yamamoto[7], Hiroyuki Mano[5], Yuichi Ishikawa[6] and Akihiko Gemma[1*]

Abstract

Background: The *EML4–ALK* (echinoderm microtubule-associated protein-like 4 gene and the anaplastic lymphoma kinase gene) fusion oncogene represents a novel molecular target in a small subset of non–small–cell lung cancers (NSCLCs). The *EML4–ALK* fusion gene occurs generally in NSCLC without mutations in epidermal growth factor receptor *(EGFR)* and *KRAS*.

Case presentation: We report that a case of *EML4–ALK*-positive NSCLC with *EGFR* mutation had a response of stable disease to both an EGFR tyrosine kinase inhibitor (EGFR-TKI) and ALK inhibitor.

Conclusions: We described the first clinical report of a patient with *EML4–ALK*-positive NSCLC with *EGFR* mutation that had a response of stable disease to both single-agent EGFR-TKI and ALK inhibitor. *EML4–ALK* translocation may be associated with resistance to EGFR-TKI, and EGFR signaling may contribute to resistance to ALK inhibitor in *EML4–ALK*-positive NSCLC.

Keywords: EML4–ALK, *EGFR* mutation, Lung cancer

Background

The *EML4–ALK* (echinoderm microtubule-associated protein-like 4 gene and the anaplastic lymphoma kinase gene) fusion oncogene was recently identified as a novel genetic alteration in non-small-cell lung cancer (NSCLC) [1]. *EML4–ALK* fusions have been detected in 2 to 7% of NSCLC patients. Patients harboring *ALK* rearrangements tend to be never and light smokers, have a history of adenocarcinoma, and be younger in age [1-6]. In general, the *EML4–ALK* fusion oncogene existed exclusively in NSCLC patients without the epidermal growth factor receptor (*EGFR*) gene mutation [1,7,8].

ALK inhibitors such as crizotinib are clinically effective in NSCLC patients harboring ALK rearrangements [9]. Crizotinib produced a high response rate and prolonged median progression-free survival among patients with ALK-positive NSCLC [9]. Crizotinib was recently approved by the US Food and Drug Administration and Japanese Ministry of Health, Labour and Welfare for the treatment of patients with advanced, ALK-rearranged NSCLC.

In this paper, we report a patient with NSCLC with concomitant ALK rearrangement and *EGFR* mutation that had a response of stable disease to both an EGFR tyrosine kinase inhibitor (EGFR-TKI) and ALK inhibitor.

Case presentation

In December 2009, a 55-year-old female who had never smoked was noted to have left lung opacity on a routine chest X-ray. No significant previous medical history was reported. Computed tomography (CT) scan of the chest revealed a 1.5 × 1.5 cm nodular lesion in the left upper lobe and hilar lymph node metastasis. Transthoracic needle biopsy histology revealed adenocarcinoma, and the histopathological subtype of the specimen was

* Correspondence: agemma@nms.ac.jp
[1]Department of Pulmonary Medicine and Oncology, Graduate School of Medicine, Nippon Medical School, Tokyo, Japan
Full list of author information is available at the end of the article

papillary adenocarcinoma with signet-ring cell components (Figure 1A-1C). The specimen was positive for periodic acid–Schiff (PAS) (Figure 1C). On immunohistochemical staining, the tumor cells were positive for thyroid transcription factor-1 (TTF-1) (Figure 1D). Laboratory findings were within normal range, except for the carcinoembryonic antigen (CEA) level of 158.0 ng/mL (normal range, 0 to 4.3 ng/mL) in the serum. She had multiple dorsal vertebra metastases (cT1N1M1b, stage IV).

Analysis for *EGFR* gene mutation was performed using a cytological specimen by means of the peptide nucleic acid–locked nucleic acid (PNA-LNA) polymerase-chain-reaction (PCR) clamp method as described previously [10,11]. The specimen showed a deletion in exon 19 (L747-A750del T751S). We collected mRNA from the same tumor specimens using Pinpoint Slide RNA Isolation System in order to clarify whether there was *EML4–ALK* (echinoderm microtubule-associated protein-like 4 gene and the anaplastic lymphoma kinase gene) fusion gene in each tumor. Reverse transcription polymerase-chain-reaction (RT-PCR) followed by direct sequencing confirmed the presence of *EML4–ALK* variant 2 [1] (Figure 2). In addition, *EML4–ALK* was identified by using fluorescent in situ hybridization (FISH) for *ALK* rearrangements (Figure 3B) and was confirmed by immunohistochemistry for ALK expression in tumor [2] (Figure 3A).

A platinum doublet was chosen as first line therapy according to existing treatment protocol in 2009. Four cycles of combination chemotherapy comprising cisplatin and pemetrexed was administered at 3-week intervals. She was judged as having a stable disease. After 7 months, spinal magnetic resonance imaging (MRI) revealed progression of the dorsal vertebra lesions. Therefore, EGFR-TKI was chosen as a 2nd-line therapy. She received gefitinib therapy at 250 mg/day administered orally for 2 months. CT imaging of the chest showed that the pulmonary nodule was not growing after gefitinib therapy, and the tumor marker levels had not changed. However, spinal MRI demonstrated growing dorsal vertebra metastases 2 months after the start of gefitinib therapy. The carcinoembryonic antigen (CEA) level increased from 117 ng/ml to 250 ng/ml. Therefore, the patient was judged as having progressive disease. After local radiation therapy with a total of 30 Gy for dorsal metastases, a second EGFR-TKI was chosen given the stable primary disease. She received another EGFR-TKI, erlotinib (150 mg/day), as 3rd-line therapy. After being progression-free for 3 months, spinal MRI revealed a growing thoracic vertebra metastasis. She received 4th-line treatment with 2 cycles of docetaxel (DTX). However, her disease progressed 6 months later. Finally, she received a targeted inhibitor of ALK. The patient initially had SD associated with a temporary decrease in the CEA level from 743 ng/ml to 520 ng/ml, but her disease progressed after 4 months of therapy. The ALK inhibitor treatment was

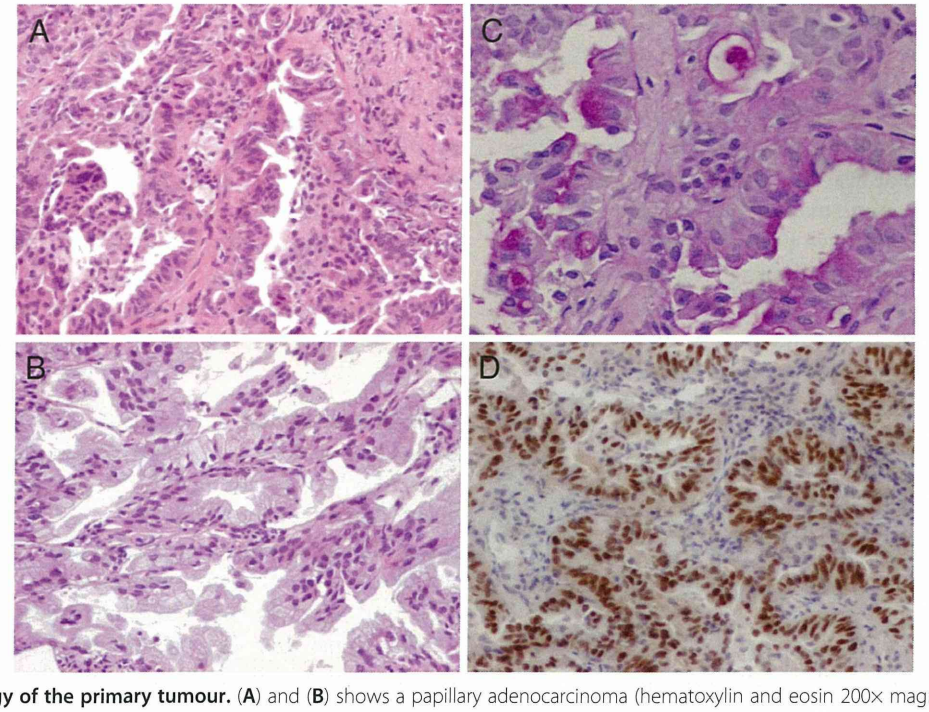

Figure 1 Histology of the primary tumour. (**A**) and (**B**) shows a papillary adenocarcinoma (hematoxylin and eosin 200× magnification), (**C**) a mucin stain shows positive for both signet-ring and papillary morphology (PAS, 400× magnification). **(D)** immunohistochemical analysis of lung adenocarcinoma specimens with *EML4-ALK* fusion using a monoclonal anti-TTF-1 antibody (200× magnification).

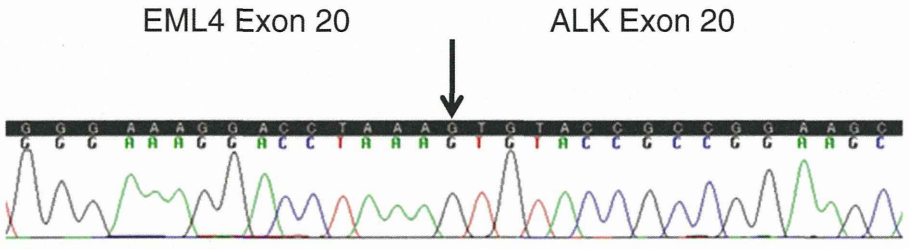

Figure 2 The sequence of the junction between *EML4* exon 20 and *ALK* exon 20.

ceased and full supportive care was given. All lines of therapy were well tolerated.

Discussion

We presented a patient with NSCLC with concomitant ALK rearrangement and *EGFR* mutation that had a response of stable disease to both EGFR-TKI and ALK inhibitors. The presence of *EML4–ALK* generally seems to be mutually exclusive of the presence of *EGFR* or *KRAS* mutations in NSCLC [1,7,8]. Previous reports showed twelve cases of *EML4–ALK*-positive lung cancer with *EGFR* mutation [3,12-17]. Only one patient with harboring *ALK* translocation and EGFR mutation was treated by ALK inhibitor has been reported [17]. Lee et al. reported two ALK-positive and EGFR-mutant NSCLC patient who did not respond to EGFR-TKI but achieved a durable partial response to ALK inhibitor [17]. The present patient was a woman with no history of smoking. Her pathological diagnosis was papillary adenocarcinoma with a signet-ring cell component, which was consistent with the previously reported characteristics of *EML4–ALK*-positive lung adenocarcinoma except for the *EGFR* mutation status [1-6]. It was reported that EGFR-TKI therapy among patients with advanced NSCLC and *EGFR* mutations revealed a response rate of more than 60% and progression-free survival of 9 to 14 months [11,18,19]. In addition, recent reports showed that ALK inhibition in NSCLC patients with the *ALK* rearrangement resulted in tumor shrinkage or stable disease in most patients [9]. Unfortunately, EGFR-TKI treatment was not effective in the tumor regression nor tumor marker level of present patient (disease might be controlled), but treatment with an ALK inhibitor resulted in SD with decreasing tumor markers. Therefore, this case showed that ALK rearrangement might be superior to EGFR mutation for the driver mutation.

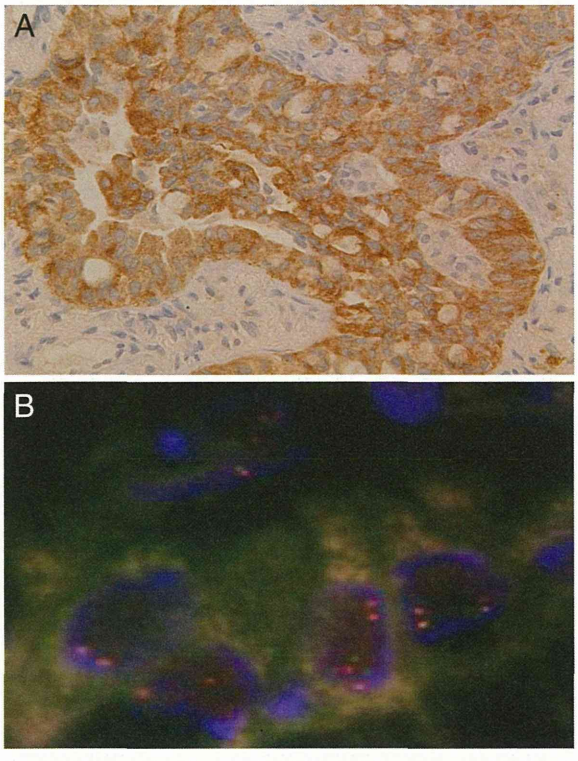

Figure 3 Diagnosis of an EML4-ALK-positive non-small cell lung cancer. (**A**) Immunostaining for ALK protein expression in tumor cells. (**B**) The results of a break-apart FISH assay of tumor cells from a patient with rearrangement of the gene encoding *ALK*.

It was reported that *EML4–ALK* fusion was associated with resistance to EGFR-TKIs [20]. Patients with NSCLC in the *EML4–ALK* cohort and the wild type cohort showed similar response rates to platinum-based combination chemotherapy and no difference in overall survival [20]. Whereas *EGFR* mutations confer sensitivity to EGFR-TKIs, *EML4–ALK* is strongly associated with resistance to EGFR-TKIs. In a previous case of concomitant *EGFR* mutation and *ALK* translocation, the patient presented the most durable response to an EGFR-TKI and was a case demonstrating no EML4–ALK expression by immunohistochemistry with an *EML4–ALK* rearrangement characterized by an isolated 3_ FISH signal [12]. Our patient presented a concurrent *EML4-ALK* rearrangement and ALK expression by immunohistochemistry; however, EGFR-TKI was not effective.

Among patients with both *EML4–ALK* rearrangement and *EGFR* mutation, *in vitro* studies showed that EGFR signaling can contribute to ALK inhibitor resistance in EML4–ALK NSCLC [14]. In addition, these findings suggested that a cancer cell line that harbors a concurrent

ALK rearrangement and an *EGFR* mutation would be expected to be resistant to both single agent ALK and EGFR inhibitors [14]. We suggest that the combination of both ALK and EGFR inhibitors as early-line treatment may represent an effective therapy for this subset of NSCLC patients.

Conclusions

This is the first clinical report of a patient with *EML4–ALK*-positive NSCLC with *EGFR* mutation that had a response of stable disease to both single-agent EGFR-TKI and ALK inhibitor. The *EML4–ALK* fusion gene defines a new molecular subset of NSCLCs with distinct clinical and pathologic features. NSCLCs with *ALK* rearrangement are highly sensitive to ALK inhibition. However, EGFR signaling may contribute to ALK inhibitor resistance in *EML4–ALK* NSCLC. Therefore, we suggest that this provides a translational opportunity whereby laboratory studies should be undertaken to understand the biological link between ALK rearrangement and *EGFR* mutation, with a view to establishing whether there is preclinical justification for using combination therapy for NSCLC with concomitant ALK rearrangement and *EGFR* mutation.

Consent

Written informed consent was obtained from the patient for publication of this case report and accompanying images.

Abbreviations

EML4: Echinoderm microtubule-associated protein-like 4; ALK: Anaplastic lymphoma kinase; NSCLC: Non-small cell lung cancer; EGFR: Epidermal growth factor receptor; TKI: Tyrosine kinase inhibitor; CT: Computed tomography; PAS: periodic acid–Schiff; TTF-1: Thyroid transcription factor-1; PNA-LNA: Peptide nucleic acid–locked nucleic acid; PCR: Polymerase chain reaction technique; FISH: Fluorescent in situ hybridization; SD: Stable disease; MRI: Magnetic resonance imaging (MRI); CEA: Carcinoembryonic antigen; RT-PCR: Reverse transcription polymerase chain reaction.

Competing interests

The authors declare that they have no competing interests.

Authors' contributions

AM prepared the manuscript and the literature search; RN and MS reviewed and edited the manuscript; HM and AG corrected and revised the manuscript; KS, KK, SK, YM, MS and TS treated and observed the patient; MK and ST performed the histopathological, immunohistochemical examinations; and AY, KH, KT, NY and YI reviewed the manuscript. All authors read and approved of the final manuscript.

Acknowledgements

The authors wish to thank Mari Masuda for technical support in the sequence alignment.

Author details

[1]Department of Pulmonary Medicine and Oncology, Graduate School of Medicine, Nippon Medical School, Tokyo, Japan. [2]Division of Diagnostic Pathology, Nippon Medical School Hospital, Tokyo, Japan. [3]Department of Clinical Pathology, University Hospital, Mizonokuchi, Teikyo University School of Medicine, Kanagawa, Japan. [4]Saitama Medical School Respiratory Organs Internal Medicine, Saitama, Japan. [5]Division of Functional Genomics, Jichi Medical University, Tochigi, Japan. [6]Division of Pathology, The Cancer Institute, Japanese Foundation for Cancer Research, Tokyo, Japan. [7]Division of Thoracic Oncology, Shizuoka Cancer Center, Shizuoka, Japan. [8]Department of Clinical Oncology, Tokyo Medical University Hospital, Tokyo, Japan.

Received: 17 January 2013 Accepted: 22 May 2013
Published: 29 May 2013

References

1. Soda M, Choi YL, Enomoto M, Takada S, Yamashita Y, Ishikawa S, Fujiwara S, Watanabe H, Kurashina K, Hatanaka H, *et al*: **Identification of the transforming EML4-ALK fusion gene in non-small-cell lung cancer.** *Nature* 2007, **448**(7153):561–566.
2. Takeuchi K, Choi YL, Soda M, Inamura K, Togashi Y, Hatano S, Enomoto M, Takada S, Yamashita Y, Satoh Y, *et al*: **Multiplex reverse transcription-PCR screening for EML4-ALK fusion transcripts.** *Clin Can Res* 2008, **14**(20):6618–6624.
3. Koivunen JP, Mermel C, Zejnullahu K, Murphy C, Lifshits E, Holmes AJ, Choi HG, Kim J, Chiang D, Thomas R, *et al*: **EML4-ALK fusion gene and efficacy of an ALK kinase inhibitor in lung cancer.** *Clin Can Res* 2008, **14**(13):4275–4283.
4. Mano H: **Non-solid oncogenes in solid tumors: EML4-ALK fusion genes in lung cancer.** *Cancer Sci* 2008, **99**(12):2349–2355.
5. Wong DW, Leung EL, So KK, Tam IY, Sihoe AD, Cheng LC, Ho KK, Au JS, Chung LP, Pik Wong M: **The EML4-ALK fusion gene is involved in various histologic types of lung cancers from nonsmokers with wild-type EGFR and KRAS.** *Cancer* 2009, **115**(8):1723–1733.
6. Perner S, Wagner PL, Demichelis F, Mehra R, Lafargue CJ, Moss BJ, Arbogast S, Soltermann A, Weder W, Giordano TJ, *et al*: **EML4-ALK fusion lung cancer: a rare acquired event.** *Neoplasia* 2008, **10**(3):298–302.
7. Inamura K, Takeuchi K, Togashi Y, Nomura K, Ninomiya H, Okui M, Satoh Y, Okumura S, Nakagawa K, Soda M, *et al*: **EML4-ALK fusion is linked to histological characteristics in a subset of lung cancers.** *J Thorac Oncol* 2008, **3**(1):13–17.
8. Shinmura K, Kageyama S, Tao H, Bunai T, Suzuki M, Kamo T, Takamochi K, Suzuki K, Tanahashi M, Niwa H, *et al*: **EML4-ALK fusion transcripts, but no NPM-, TPM3-, CLTC-, ATIC-, or TFG-ALK fusion transcripts, in non-small cell lung carcinomas.** *Lung Cancer* 2008, **61**(2):163–169.
9. Kwak EL, Bang YJ, Camidge DR, Shaw AT, Solomon B, Maki RG, Ou SH, Dezube BJ, Janne PA, Costa DB, *et al*: **Anaplastic lymphoma kinase inhibition in non-small-cell lung cancer.** *N Engl J Med* 2010, **363**(18):1693–1703.
10. Nagai Y, Miyazawa H, Huqun, Tanaka T, Udagawa K, Kato M, Fukuyama S, Yokote A, Kobayashi K, Kanazawa M, *et al*: **Genetic heterogeneity of the epidermal growth factor receptor in non-small cell lung cancer cell lines revealed by a rapid and sensitive detection system, the peptide nucleic acid-locked nucleic acid PCR clamp.** *Cancer Res* 2005, **65**(16):7276–7282.
11. Maemondo M, Inoue A, Kobayashi K, Sugawara S, Oizumi S, Isobe H, Gemma A, Harada M, Yoshizawa H, Kinoshita I, *et al*: **Gefitinib or chemotherapy for non-small-cell lung cancer with mutated EGFR.** *N Engl J Med* 2010, **362**(25):2380–2388.
12. Popat S, Vieira de Araujo A, Min T, Swansbury J, Dainton M, Wotherspoon A, Lim E, Nicholson AG, O'Brien ME: **Lung adenocarcinoma with concurrent exon 19 EGFR mutation and ALK rearrangement responding to erlotinib.** *J Thorac Oncol* 2011, **6**(11):1962–1963.
13. Tiseo M, Gelsomino F, Boggiani D, Bortesi B, Bartolotti M, Bozzetti C, Sammarelli G, Thai E, Ardizzoni A: **EGFR and EML4-ALK gene mutations in NSCLC: a case report of erlotinib-resistant patient with both concomitant mutations.** *Lung Cancer* 2011, **71**(2):241–243.
14. Sasaki T, Koivunen J, Ogino A, Yanagita M, Nikiforow S, Zheng W, Lathan C, Marcoux JP, Du J, Okuda K, *et al*: **A novel ALK secondary mutation and EGFR signaling cause resistance to ALK kinase inhibitors.** *Cancer Res* 2011, **71**(18):6051–6060.
15. Tanaka H, Hayashi A, Morimoto T, Taima K, Tanaka Y, Shimada M, Kurose A, Takanashi S, Okumura K: **A case of lung adenocarcinoma harboring EGFR mutation and EML4-ALK fusion gene.** *BMC Cancer* 2012, **12**(1):558.
16. Kuo YW, Wu SG, Ho CC, Shih JY: **Good response to gefitinib in lung adenocarcinoma harboring coexisting EML4-ALK fusion gene and EGFR mutation.** *J Thorac Oncol* 2010, **5**(12):2039–2040.
17. Lee JK, Kim TM, Koh Y, Lee SH, Kim DW, Jeon YK, Chung DH, Yang SC, Kim YT, Kim YW, *et al*: **Differential sensitivities to tyrosine kinase inhibitors in NSCLC harboring EGFR mutation and ALK translocation.** *Lung Cancer* 2012, **77**(2):460–463.

18. Fukuoka M, Wu YL, Thongprasert S, Sunpaweravong P, Leong SS, Sriuranpong V, Chao TY, Nakagawa K, Chu DT, Saijo N, *et al*: Biomarker analyses and final overall survival results from a phase III, randomized, open-label, first-line study of gefitinib versus carboplatin/paclitaxel in clinically selected patients with advanced non-small-cell lung cancer in Asia (IPASS). *J Clin Oncol* 2011, **29**(21):2866–2874.
19. Mitsudomi T, Morita S, Yatabe Y, Negoro S, Okamoto I, Tsurutani J, Seto T, Satouchi M, Tada H, Hirashima T, *et al*: Gefitinib versus cisplatin plus docetaxel in patients with non-small-cell lung cancer harbouring mutations of the epidermal growth factor receptor (WJTOG3405): an open label, randomised phase 3 trial. *Lancet Oncol* 2010, **11**(2):121–128.
20. Shaw AT, Yeap BY, Mino-Kenudson M, Digumarthy SR, Costa DB, Heist RS, Solomon B, Stubbs H, Admane S, McDermott U, *et al*: Clinical features and outcome of patients with non-small-cell lung cancer who harbor EML4-ALK. *J Clin Oncol* 2009, **27**(26):4247–4253.

doi:10.1186/1471-2407-13-262
Cite this article as: Miyanaga *et al.*: Activity of EGFR-tyrosine kinase and ALK inhibitors for *EML4–ALK*-rearranged non–small–cell lung cancer harbored coexisting *EGFR* mutation. *BMC Cancer* 2013 13:262.

Ninomiya et al. BMC Cancer 2013, 13:8
http://www.biomedcentral.com/1471-2407/13/8

BMC Cancer

RESEARCH ARTICLE Open Access

Allelotypes of lung adenocarcinomas featuring *ALK* fusion demonstrate fewer onco- and suppressor gene changes

Hironori Ninomiya[1], Motohiro Kato[4,5], Masashi Sanada[4], Kengo Takeuchi[1,2], Kentaro Inamura[1], Noriko Motoi[1], Hiroko Nagano[1], Kimie Nomura[1], Yukinori Sakao[3], Sakae Okumura[3], Hiroyuki Mano[6,7], Seishi Ogawa[4] and Yuichi Ishikawa[1*]

Abstract

Background: A subset of lung adenocarcinomas harboring an *EML4-ALK* fusion gene resulting in dominant oncogenic activity has emerged as a target for specific therapy. *EML4-ALK* fusion confers a characteristic histology and is detected more frequently in never or light smokers and younger patients.

Methods: To gain insights into etiology and carcinogenic mechanisms we conducted analyses to compare allelotypes of 35 *ALK* fusion-positive and 95 -negative tumours using single nucleotide polymorphism (SNP) arrays and especially designed software which enabled precise global genomic profiling.

Results: Overall aberration numbers (gains + losses) of chromosomal alterations were 8.42 and 9.56 in tumours with and without *ALK* fusion, respectively, the difference not being statistically significant, although patterns of gain and loss were distinct. Interestingly, among selected genomic regions, oncogene-related examples such as 1p34.3 (*MYCL1*), 7q11.2(*EGFR*), 7p21.1, 8q24.21(*MYC*), 16p13.3, 17q12(*ERBB2*) and 17q25.1 showed significantly less gain. Also, changes in tumour suppressor gene-related regions, such as 9p21.3 (*CDKN2A*) 9p23-24.1 (*PTPRD*), 13q14.2 (*RB1*), were significantly fewer in tumours with *ALK* fusion.

Conclusion: Global genomic comparison with SNP arrays showed tumours with *ALK* fusion to have fewer alterations in oncogenes and suppressor genes despite a similar overall aberration frequency, suggesting very strong oncogenic potency of *ALK* activation by gene fusion.

Keywords: Lung adenocarcinoma, *ALK* fusion, SNP array, Allelotype, Copy number

Background

The adenocarcinoma is the most common form of lung cancer worldwide, different subsets having specific genetic backgrounds of great importance for molecular-targeted therapy. For example, somatic mutations of the epidermal growth factor receptor (*EGFR*) are especially prevalent in adenocarcinomas among never smokers, females, and those with Asian ethnicity [1]. On the other hand, *KRAS* mutations are associated with the smoking habit [2] and the two tend to be mutually exclusive. Recently, Soda et al. found a novel fusion gene, *EML4-ALK*, arising from an inversion on the short arm of chromosome 2 in non-small cell lung carcinomas [3]. *ALK* fusion is a unique example of tyrosine kinase activation by structural chromosome rearrangement [4].

EML4-ALK fusion is a powerful driving molecular event by itself. The chimeric protein permits ligand-independent dimerization and constitutive activation of *ALK*, resulting in dominant oncogenic activity. Multiple fusion variants of *EML4-ALK* and notable clinicopathological characteristics of fusion positive tumours have been revealed [5-9]. Since the tyrosine kinase is involved and activated by gene fusion, this type of malignancy has emerged as a target for anti-tyrosine kinase therapy [4,10-12].

We have revealed that *ALK* fusion-positive tumours constituted a particular subset in lung adenocarcinomas in

* Correspondence: ishikawa@jfcr.or.jp
[1]Division of Pathology, The Cancer Institute, Ariake 3-8-31, Koutou-ku, Tokyo 135-8550, Japan
Full list of author information is available at the end of the article

terms of clinical characteristics, histology and etiology, as well as molecular changes [7,8]. It is of great interest to assess global genomic alterations to provide deep insight into their genesis, especially considering these tumours arise in non- or light smokers. Single nucleotide polymorphism (SNP) microarray analysis enables precise high-throughput detection of genomic copy number alterations, gains and losses in the genome contributing to carcinogenesis [13] with gene expression varying consistently with DNA copy number changes [14,15]. We therefore conducted of the present genomic profiling of lung adenocarcinomas with and without *ALK* fusion.

Methods

Patient population and specimens

A series of 130 cases of lung adenocarcinomas, 35 with *EML4-ALK* or *KIF5B-ALK* fusion and 95 cases without, were enrolled in this study. From 1998 to 2008, 1,086 primary lung adenocarcinomas were surgically resected at Thoracic Surgery Division, the Cancer Institute Hospital, Japanese Foundation for Cancer Research (JFCR), Tokyo. All cases were screened as to ALK expression by immunohistochemistry using the iAEP method [6] and for positive cases subsequent RT-PCR and FISH analysis were performed, as previously described [5,6,16]. Among them, sufficient amounts and quality of fresh tumour material were available for 35 cases. Fusion gene variants are listed in Addtional file 1: Table S1. V3 constituted the largest proportion, 31% (11/35), having a breakpoint at exon 20 of *EML4*. A rare variant, *KIF5B-ALK* fusion, was detected in two cases. There was no correlation with fusion variant and pathological subtypes (data not shown). The 95 cases without *ALK* fusion were randomly selected from 730 surgically resected adenocarcinomas from 1995 to 2003 at the same hospital. Tissue specimens were snap-frozen in liquid nitrogen, typically within 20 minutes after resection, and stored at −80°C until use. Genomic DNA was extracted by standard proteinase K digestion and the phenol-chloroform method. To confirm if specimens used for analysis in this study contained a significant amount of tumour cells, typically 50% or more, a neighboring surface was examined histologically with frozen sections. This study was approved by the institutional review board of the JFCR.

Mutation analysis of EGFR, KRAS and TP53

For *EGFR* mutation analysis, exons 18 to 21 were amplified by PCR with specific oligo-primers. For point mutations in exon 18, PCR products were directly sequenced. Fragment analysis was performed for exons 19 and 20 deletions and insertion mutations. The presence of one point mutation in exon 21 was detected by genotyping analysis. To examine *TP53* mutations, direct sequencing from exons 5 to 10 was carried out. For *KRAS* mutation analysis, codons 12, 13 and 61 were examined by direct sequencing. Primers and detailed procedures were as described previously [17].

Histological diagnosis and clinical staging

Histological diagnosis was made on the basis of World Health Organization (WHO) classification [18] by experienced pathologists (N.M. and Y.I.). Pathological staging was based on the AJCC/UICC staging manual of lung cancer [19]. Differentiation grading of adenocarcinoma was determined essentially according to the Japan Lung Cancer Society criteria as illustrated previously [20]. Briefly, well-differentiated (w/d) tumors are composed chiefly of glands lined by, or of papilla covered by, one-layered tumor cells. Also, Adenocarcinoma in situ (AIS) is included in this category. Moderately differentiated (m/d) lesions comprise glands showing a cribriform pattern, fused with one another, or glands lined by, or papillae covered by, tumor cells demonstrating obvious piling-up. Poorly differentiated (p/d) carcinomas show mainly solid growth and only occasionally glandular/papillary patterns and/or mucus production. Blood vessel and lymphatic invasion was also explored microscopically, with hematoxylin-eosin and elastic-fiber stained sections of maximum tumour diameter made from paraffin-embedded specimens.

SNP array analysis and comparisons of allelic imbalance at the chromosome arm level and in selected cancer-related regions

Extracted DNA was subjected to Affymetrix GeneChip Mapping 250K arrays. Allelic imbalance was analyzed using software termed the Copy Number Analyzer for Affymetrix Gene Chip Mapping (CNAG Ver. 2.0) [21]. After appropriate normalization of mean array intensities, signal ratios between tumours and anonymous normal references were calculated in an allele-specific manner, and allele-specific copy numbers were inferred from the observed signal ratios based on the hidden Markov model using the CNAG/AsCNAR software [21-23]. With this procedure, genomic profiles of *ALK* fusion-positive and -negative tumours were obtained. Datas have been deposited at NCBI's Gene Expression Omnibus data repository under GEO series accession number GSE41536.

Comparison was at two levels; a chromosome arm level and a smaller, specific gene locus level. To do this, first we compared average numbers of chromosome arms altered between the two groups [24]. We called gain or loss of each chromosomal arm when copy number change stretched more than 80% of entire length. Secondly, we compared recurrent copy number aberrations at twenty-one cancer-related loci with gains and five with losses. These specific regions were selected based on previous studies of the lung cancer genome

[25,26] and through our global mapping with CNAG. The selected regions with relevant genes were as follows: for gains, 1p34.3 (*MYCL1*), 1q21.2 (*S100 family*), 3q29 (*MUC4*), 5p15.33 (*TERT*), 6p21.1 (*VEGF*), 7p11.2 (*EGFR*), 7p21.1, 7q31.2 (*MET*), 8q24.21 (*MYC*), 10q11.22, 12p12.1 (*KRAS*), 12q14.1 (*CDK4*), 12q15 (*MDM2*), 14q13.3 (*TTF1*), 16p13.3, 17q12 (*ERBB2*), 17q25.1, 19q12 (*CCNE1*), 20q13.2, 20q13.32, 20q13.33 (*TNFSF6B*); and for losses, 9p21.3 (*CDKN2A*), 9p23-p24.1 (*PTPRD*), 10q23.31 (*PTEN*), 13q14 (*RB1*), 17p13.1 (*TP53*).

Statistical analysis

Clinicopathological parameters of cases with or without *ALK* fusion and the frequencies of chromosome arms changed and copy numbers of targeted loci were compared by the chi-square test or the Fisher's exact test as appropriate. The average number of chromosome arms altered with or without *ALK* fusion was compared with Students' *t*-test. Statistical significance was defined as P=0.05 or less.

Results

Comparisons of clinicopathological profiles of tumours with or without *ALK* fusion

Clinicopathological profiles of patients are summarized in Table 1. *ALK* fusion-positive cases were significantly younger and featured significantly more never-smokers (P=0.05, P=0.004, respectively). *ALK* fusion-positive tumours were histologically adenocarcinomas with notable characteristics such as poor differentiation as well as an acinar type structure and mucin production, as reported previously [7-9]. In this study, distribution of histological subtypes differed between two groups, namely, "acinar" subtype accounted for nearly forty percent in *ALK* fusion positive group (Table 1). The frequencies of vascular invasion, both of blood and lymph vessels, did not significantly differ between the two groups (P=0.738, P=0.273, respectively). In addition, the distribution of pathological stages did not vary (P=0.532).

Mutational status of TP53, EGFR and KRAS

Data for the mutational status of *TP53, EGFR and KRAS* in the two groups are summarized in Table 1. Twenty-one cases had *TP53* mutations. Only one case with *ALK* fusion (Case 9: 1/35, 3%) harbored a mutation, a G/A transition at codon 273, as compared to 20 cases without *ALK* fusion (20/95, 21%), the mutation rates being significantly different (P=0.014) (Table 1, Additional file 1: Table S2). Twelve (12/21, 57%) of the *TP53*-mutated cases had a smoking history.

EGFR and *KRAS* mutations were not detected among *ALK* fusion-positive tumours. This fact that *ALK* rearrangement was mutually exclusive with *EGFR* and *KRAS* mutations (P<0.0001, P=0.189, respectively) is in line with our previous studies [8]. The *EGFR* mutation rate was 58% (55/95) in *ALK* fusion-negative cases and decreased with the smoking burden: 70.7% (29/41) in never smokers, 62.5% (15/24) in light smokers (0<pack-years<20) and 36.7% in heavy smokers (more than 20 pack-years) (11/30) (Additional file 2: Figure S1). *KRAS* mutations were identified in 7.4% (7/95) of *ALK* fusion-negative cases, and detected only among smokers. Though *KRAS* mutations were examined through

Table 1 Comparison of clinicopathological parameters in cases with or without ALK fusion

	with fusion	without fusion	*P*
n	35	95	
Age (years)	58.5	62.8	0.050
gender			
male	14	47	0.337
female	21	48	
smoking			
never	25	41	0.004
ever	10	54	
pStage			
I	20	60	0.532
II-IV	15	35	
differentiation grade			
wel	4	44	<0.001
mod+por	31	51	
Predominant subtype			
papillary	21	77	0.019
Acinar	13	13	
Bronchioloalveolar	0	4	
solid with mucin	0	1	
signet	1	0	
lymphatic invasion			
-	24	68	0.738
+	11	27	
Vessel invasion			
-	15	51	0.273
+	20	44	
TP53 mutation			
-	34	75	0.014
+	1	20	
EGFR mutation			
-	35	40	<0.0001
+	0	55	
KRAS mutation			
-	35	88	0.189
+	0	7	

codons 12, 13 and 61, they were found only in codon 12. The *KRAS* mutation rate increased along with the elevation of smoking index (Additional file 2: Figure S1). These findings for *EGFR* and *KRAS* mutations are consistent with previous reports from Japan, the prevalence being quite different from that in the United States [27-29].

DNA copy number alterations of chromosome arms

We compared the allelotypes of each chromosome arm between the two groups. Global views of chromosome aberrations are shown in Figure 1. Note that in *ALK* fusion-positive tumours, genomic copy number changes were more evenly distributed over the chromosome arms and high copy number gains (dark-red) in short genomic segments were less frequently encountered than with *ALK*-fusion negative examples. Significantly different patterns of respective chromosomal arm gain and loss were noted between the two groups. In fact, 5q, 8p, 9q, 11p and 11q were significantly more amplified, and 6q was more deleted in *ALK* fusion-positive tumours, whereas, in *ALK* fusion-negative tumours, 17q was more amplified, and 8p and 9p were more deleted (Figure 1, Table 2a, Additional file 1: Table S3-S5). *P*-values for comparisons of the aberration frequency in each chromosome arms are shown in Additional file 1: Table S5. When comparing global chromosome instability levels between the two groups, average numbers of chromosome arms with copy number gain or loss were 8.42 ±7.46 and 9.56 ±7.90 for tumours with and without *ALK* fusion, respectively, as detailed in Table 3, the difference not being statistically significant.

Chromosomal number alterations with advancement of pathological stage

Chromosome aberration might be expected to increase as tumours progress in stages and, if so, numbers of chromosome arms with gain and/or loss might be larger in advanced tumours. In fact however, when we compared the number of chromosome arm altered between pathological stage I and II-IV, total number did not increase in pathological stage II-IV, though only *ALK* fusion-negative tumours showing significant elevation of chromosomal gain (Figure 2).

Comparison of gain and loss frequency of selected loci

We selected twenty-one loci with recurrent copy number gain and five loci with loss to compare small-scale genomic aberrations. All the loci examined and *P*-values are summarized in Additional file 1: Table S6, S7. In Figure 3, stacked bar charts are shown indicating the

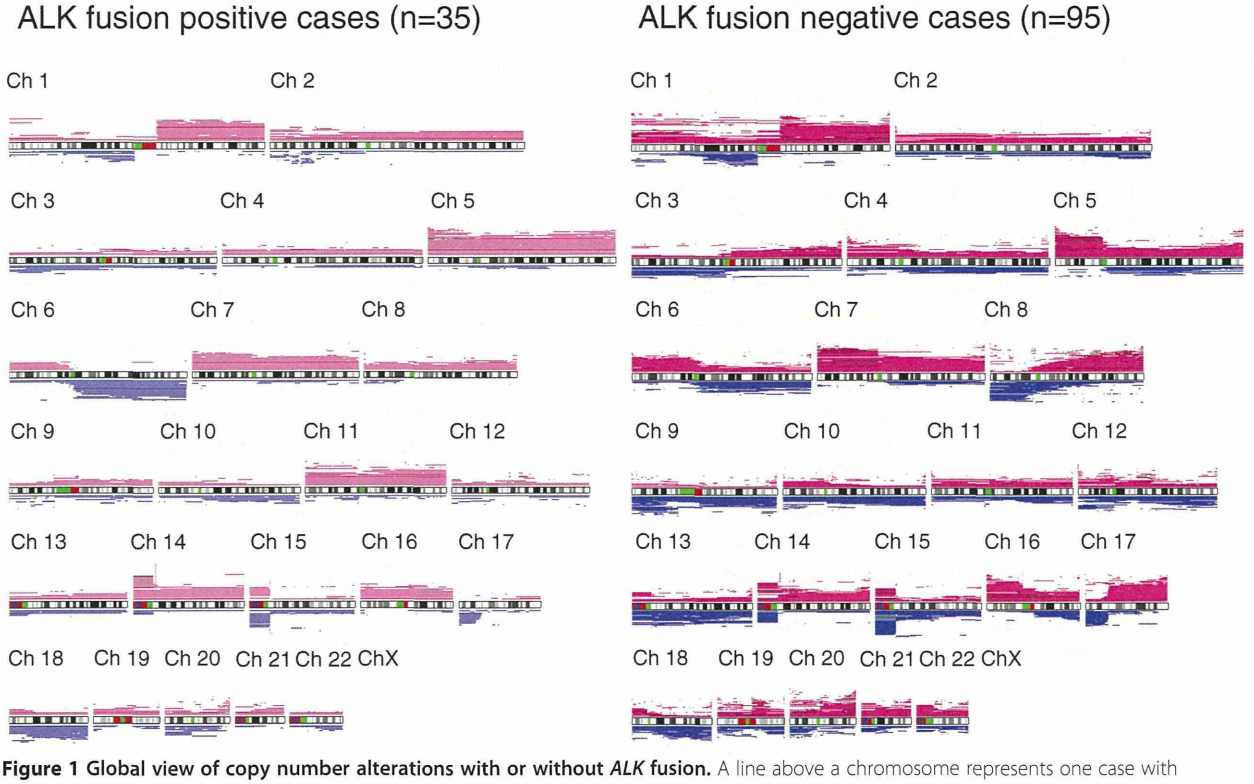

Figure 1 Global view of copy number alterations with or without *ALK* fusion. A line above a chromosome represents one case with genomic gain and its length. The color indicates the copy number of genomic regions: pink, 3 or 4 copies; and dark-red, ≥ 5 copies. Lines beneath the chromosomes represent copy number loss: blue, 1 copy; and light-green, 2 copies (homozygous deletion). Width between the lines of the two groups are adjusted according to the number of cases included for ease of visual comparison.

Table 2 Comparisons of significantly altered chromosomal arms between adenocarcinomas with and without *ALK* fusion

Category	Gain	Loss
More frequent *with* ALK fusion	5q, 8p, 9q, 11p, 11q	6q
More frequent *without* ALK fusion	17q	8p, 9q

percentage gain or loss of the selected loci. Interestingly, copy numbers (and related genes) at 1p34.3 (*MYCL1*), 7p11.2 (*EGFR*), 7p21.1, 8q24.21 (*MYC*), 16p13.3, 17q12 (*ERBB2*) and 17q25.1 were significantly less gained, and those at 9p21.3 (*CDKN2A*), 9p23-p24.1 (*PTPRD*), 13q14.2 (*RB1*) were significantly less deleted in *ALK* fusion-positive tumours than fusion-negative ones, with loci related to both oncogenes and tumour suppressor genes having fewer changes in tumours with *ALK* fusion. There were no oncogene-related loci with more gains and no suppressor gene-related loci with more losses in tumours with *ALK* fusion.

Homozygous deletions were found only at 9p21, at frequencies similar between the two groups, although the summed frequencies of heterozygous and homozygous deletions at 9p21.3 did significantly differ. In the group without *ALK* fusion, all the cases with the homozygous deletion harbored *EGFR* mutations.

MYCL1, EGFR, MYC and *ERBB2* are well-known oncogenes and *CDKN2A* and *RB1* are tumour suppressor genes related to lung carcinogenesis. *PTPRD* has been suggested to function as a tumour suppressor in several tumours, including lung cancers [30] and brain tumours [31]. Notably, 5p15.33, including *TERT* (telomerase reverse transcriptase), had the highest rate of gain in both groups regardless of *ALK* fusion (Additional file 3: Figure S2 and Additional file 1: Table S7).

Taken together, *ALK* fusion-positive tumours showed similar levels of overall chromosome instability, but when focusing on particular cancer-related regions, significantly fewer copy number gains at oncogene-related loci and significantly fewer deletions at suppressor gene-related loci.

Discussion

Recurrent chromosome translocation has been accepted to play an important role in the pathogenesis of hematological malignancies, but not of solid tumours. Recently, however, chromosome rearrangements in solid tumours such as prostate cancer and non-small cell lung cancer have been reported [32]. *ALK* fusion was originally described in anaplastic large-cell lymphoma as a chimeric protein *NPM-ALK* resulting from a translocation. More recently, evidence has accumulated that the *EML4-ALK* fusion gene defines a novel subclass of lung adenocarcinomas with distinct clinicopathological features [7-9], so that it has emerged as a target for therapy. We focused here for the first time on allelic imbalance of tumours with *ALK* fusion with a novel technique which has already shown the involvement of loss of A20 function in the pathogenesis of a subset of B-cell lymphomas [33] and gain of function of C-CBL tumour suppressor in myeloid neoplasms [34]. Applying this methodology, we demonstrated that lung adenocarcnomas with *ALK* fusion feature less amplification of loci with oncogenes and fewer deletions of loci related to tumour suppressor genes, although global chromosome aberrations were similar between tumours with and without *ALK* fusion. suggesting that the fusion gene is a driver mutation, not just a passenger mutation.

Table 3 Comparisons of numbers of chromosome arms with aberrations between adenocarcinomas with or without *ALK* fusion

	with *ALK* fusion (n=35)	without *ALK* fusion (n=95)	*P*
Gains	5.97±6.75	6.21±6.95	0.859
Losses	2.46±3.06	3.35±4.34	0.196
Total	8.42±7.46	9.56±7.90	0.454

Note that significant differences are not detected.

Genetic instability was here categorized into two groups for simplicity, at the chromosomal level and at the nucleotide level. We earlier found the former to play a more important role in lung carcinogenesis, the frequency of LOH (loss of heterozygosity) being higher in less-differentiated tumours [35]. *ALK* fusion positive tumours are more common among non-smokers and the younger population, similar to those with *EGFR* mutations. We had expected fewer chromosome aberrations in *ALK* fusion-positive tumours because tumours arising in such people usually harbor less LOH and a lower *TP53* mutation rate than smokers [36-38]. Contrary to our expectation, the global copy number changes at the chromosomal arm level did not differ between the two groups, although significant differences of alteration frequency at the individual chromosomal arms were seen. In addition, only *ALK* fusion-negative tumours showed an increase of the frequency of chromosome arm gain with the advancement of disease stage. Furthermore, at the smaller-genomic scale level, *ALK* fusion-positive tumours were less amplified at the loci containing *EGFR* family genes, 7p11.2 (*EGFR*), 17q12 (*ERBB2*) and other loci, 1p34.3 (*MYCL*), 7p21.1, 8q24.21 (*MYC*), 16p13.3 and 17q25.1. *EGFR* and *ERBB2* play important roles by dimerizing when their ligands binds to produce downward growth signals to the tumour cells. Mutations and activation of these genes may drive carcinogenesis [39], and increased expression is associated with a poor prognosis in NSCLCs [40-43]. *ALK* fusion positive tumours are speculated to be less dependent on the actions of oncogenes and tumour-suppressor genes induced by copy number changes. Our results may also indicate that there

	p-Stage	with *ALK* fusion	*P*	without *ALK* fusion	*P*
Gain	I	5.05±6.07	n.s.	4.97±6.41	0.017
	II-IV	7.20±7.59		8.53±7.43	
Loss	I	1.90±3.11	n.s.	3.60±4.66	n.s.
	II-IV	3.20±2.93		2.88±3.80	
Gain +Loss	I	6.95±6.78	n.s.	8.57±7.71	n.s.
	II-IV	10.4±8.09		11.41±8.11	

Figure 2 Comparisons of numbers of chromosome arms altered with or without *ALK* fusion in different pathological stages. Note that, whereas tumours in higher stages show more gains than stage I tumours when the tumours have no *ALK* fusion, *ALK* fusion positive tumours exhibit no such difference. p-Stage; pathological stage, n.s.; not statistically significant.

is common and frequent chromosome abnormality in lung adenocarcinomas independent of *ALK* fusion, such as the 5p15.33 region, including *TERT*.

As for genomic loss, 9p21.3 (*CDKN2A*), 9p23-p24.1 (*PTPRD*) and 13q14.2 (*RB1*) were significantly less frequently deleted in *ALK* fusion-positive tumours. Homozygous deletion was seen only at 9p21.3 including *CDKN2A* and limited to *EGFR*-mutated tumours among *ALK* fusion-negative neoplasms as reported in the literature [44] and also seen in *ALK*-fusion positive ones. That deletion of 9p23-24.1 and 13q14.2 including tumour suppressor genes was rare in *ALK* fusion-positive tumours suggests that they can grow even if the functions of these suppressor genes are retained.

Of all the selected loci, 5p15.33 containing *TERT* (telomerase reverse transcriptase isoform 2) showed the highest frequency of recurring gain regardless of *ALK* fusion. The enzyme is important for telomere regeneration and maintenance resulting in a growth advantage and Zhang et al. reported that the locus is a frequent target of amplification during tumourigenesis [45]. Copy number gain of this locus significantly correlates with telomerase activity [46] and is one of the most consistent alterations in the early stages of non-small cell lung cancer [47]. In addition, increased susceptibility to lung cancer development associated with a SNP polymorphism of this locus has been reported [48,49]. The fact that most human tumour cells have telomerase activity indicates that its acquisition is vital for carcinogenesis and cell immortalization, and it might explain the reason why lung adenocarcinomas with or without *ALK* fusion shows similar frequency of copy number gain of this locus.

Our results have some therapeutic relevance. The fact that there are less involvement of other oncogenes and tumor suppressor genes may be related to dramatic responses to targeted drugs because of intact cellular processes including apoptosis pathways. In this regard, there is an interesting paper by Camidge et al. [50], demonstrating the inverse relationship between fused and isolated red copy number on FISH might suggest

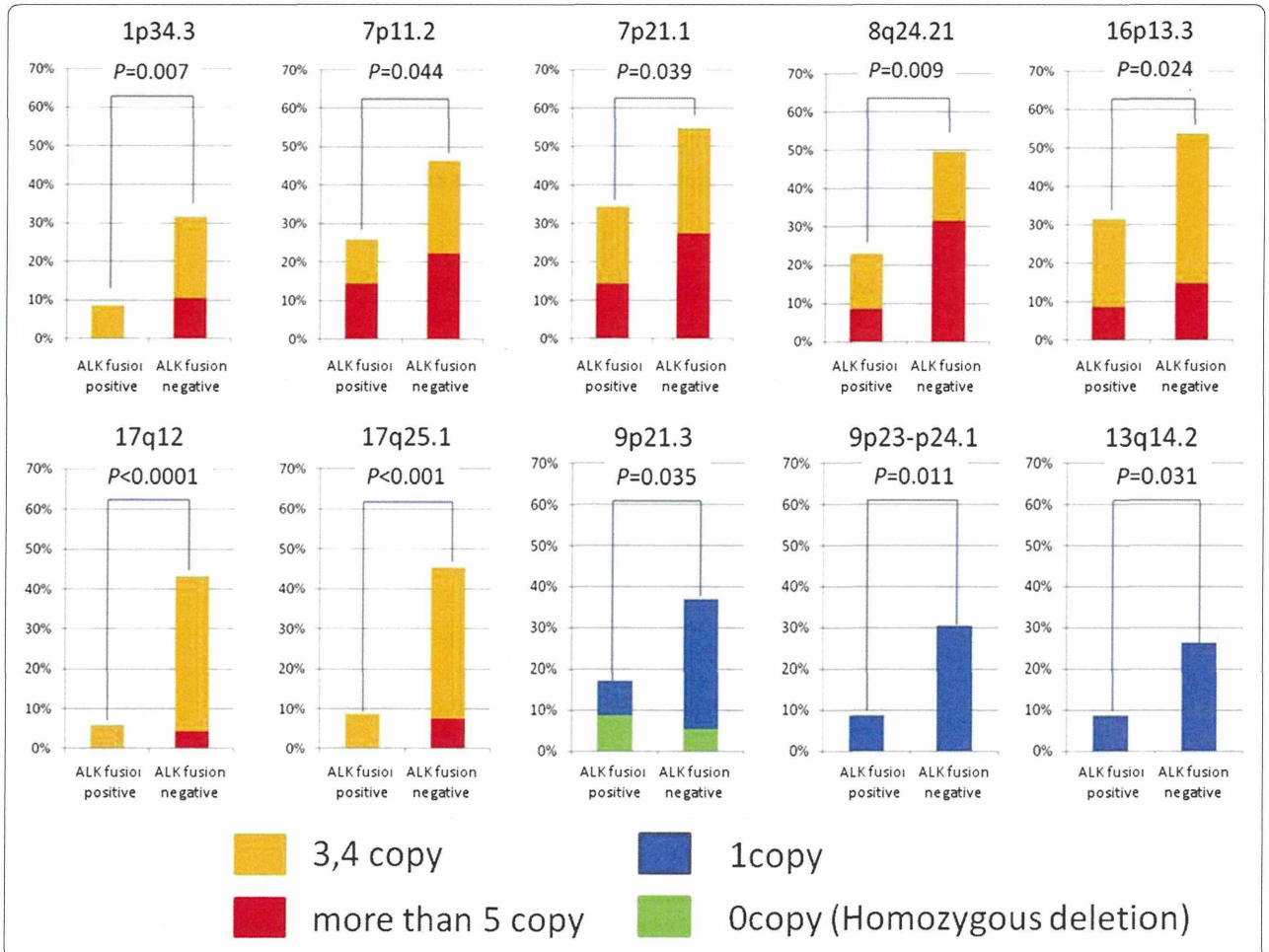

Figure 3 Significant differences in copy number change detected at seven loci for gain and three loci for loss among twenty-six selected loci. Colors of the stacked bars represent copy number: orange, 3,4 copies; red, ≥ 5 copies; blue, 1 copy loss (heterozygous deletion), light green: 2 copy losses (homozygous deletion). 17q12, 17q25.1 show remarkable differences in copy number gain between *ALK* fusion-positive and -negative tumours.

the *ALK* fusion positive tumor was a "near-diploid" subtype of non-small cell lung cancer. Comparing closely, however, between their and our results, our study clearly revealed the overall frequency of chromosome aberrations are similar between *ALK* fusion positive and negative tumors, suggesting not "near-diploid". But, certainly, we need more investigations on genomic instability of *ALK* fusion positive tumors.

It is well known that smoking causes genomic changes with allelic imbalance [20]. As shown in Table 1, smokers dominate never smokers in the group without fusion whereas the fusion-positive group has more never smokers than smokers. Since the tumors without *ALK* fusion include *EGFR*-mutated tumors, most of which are from never smokers, the *ALK* fusion-negative group is certainly heterogeneous. In due course, a study that describes comparisons of allelotypes of non-smoker's tumors between with *ALK* fusion and with *EGFR* mutation should be warranted.

Conclusions

Although overall frequencies of aberrations at the chromosome arm level do not appear to significantly differ between *ALK* fusion-positive and -negative tumors, smaller genomic regions including cancer-related genes do show significant variation. Thus tumors with *ALK* fusion feature significantly fewer copy number gains and losses at loci containing oncogenes and tumor-suppressor genes, respectively. This implies that *ALK* fusion itself exerts very strong driving forces for tumorigenesis, in other words, that *ALK* fusion is a driver mutation, not just a passenger mutation.

Additional files

Additional file 1: Table S1. Frequencies of fusion variants of *ALK* rearrangements. **Table S2.** Cases with *TP53* mutations and their smoking status. **Table S3.** Chromosomal arms and number of cases with gain with or without ALK fusion. **Table S4.** Chromosomal arms and number

of cases with loss with or without ALK fusion. **Table S5.** P-values for comparisons of the frequencies of chromosome aberrations in all chromosome arms between tumours with or without *ALK* fusion. **Table S6.** Number of cases with copy number gain or loss at selected loci with or without *ALK* fusion. **Table S7.** Significance of the differences in frequencies of copy number changes (gains and losses) between tumours with or without *ALK* fusion.

Addtional file 2: Figure S1. Mutation rates for EGFR, TP53 and KRAS according to cumulative smoking are shown. EGFR and KRAS mutations were only detected among ALK fusion negative cases, so ALK fusion positive cases were not included in the analysis. Note the gradually decrease in EGFR mutation rate with increase in cumulative smoking. KRAS mutations were detected only among smokers.

Additional file 3: Figure S2. Comparisons of copy number alteration rates at selected loci with or without *ALK* fusion. Note that 5p15.33 including *TERT* shows the highest gain both in *ALK* fusion positive and negative tumours, the frequencies being identical.

Competing interest
The authors have no potential conflicts of interest.

Authors' contributions
HN, MK, SO, HM and YI designed the study. HN, KT, KI, NM, HM and YI performed pathological and/or genomic diagnosis of tumors. HN, MK, MS and SO obtained microarray data and carried out bioinformatics analysis. HN and KN analyzed mutations. YS, SO and YI collected samples and/or provided detailed clinical data of patients. HN and YI drafted the manuscript. All authors read and approved the final manuscript.

Authors' information
HM has found ALK fusion in lung cancer with own developed cDNA library. MK, MS and SO detected genes responsible for hematological disorders through same algorithm with this study, CNAG/AsCAR. KT has created a novel diagnostic method to detect *ALK* fusion positive lung cancer. YI has found characteristic pathological features of *ALK* positive cancer.

Acknowledgements
We would like to express my gratitude to Satoko Baba for assistance in sample preparation and Yuki Takano for secretary work. This work was supported by Grants-in-Aid for Scientific Research from the Ministry of Education, Culture, Sports, Science and Technology, Japan, from Japan Society for the Promotion of Science, grants from the Ministry of Health, Labour and Welfare, the Japan Science and Technology Agency, and the Smoking Research Foundation.

Author details
[1]Division of Pathology, The Cancer Institute, Ariake 3-8-31, Koutou-ku, Tokyo 135-8550, Japan. [2]Pathology Project for Molecular Targets, The Cancer Institute, Ariake 3-8-31, Koutou-ku, Tokyo 135-8550, Japan. [3]Thoracic Oncology Center, Cancer Institute Hospital, Japanese Foundation for Cancer Research, Ariake 3-8-31, Koutou-ku, Tokyo 135-8550, Japan. [4]Cancer Genomics Project, The University of Tokyo, Hongo 7-3-1, Bunkyo-ku, Tokyo 113-8656, Japan. [5]Department of Pediatrics, The University of Tokyo, Hongo 7-3-1, Bunkyo-ku, Tokyo 113-8656, Japan. [6]Department of Medical Genomics, Graduate School of Medicine, The University of Tokyo, Hongo 7-3-1, Bunkyo-ku, Tokyo 113-8656, Japan. [7]Division of Functional Genomics, Jichi Medical University, Tochigi 329-0498, Japan.

Received: 6 April 2012 Accepted: 18 December 2012
Published: 5 January 2013

References
1. Shigematsu H, Lin L, Takahashi T, Nomura M, Suzuki M, Wistuba II, Fong KM, Lee H, Toyooka S, Shimizu N, Fujisawa T, Feng Z, Roth JA, Herz J, Minna JD, Gazdar AF: **Clinical and biological features associated with epidermal growth factor receptor gene mutations in lung cancers.** *J Natl Canc Inst* 2005, **97**:339–346.
2. Mounawar M, Mukeria A, Le Calvez F, Hung RJ, Renard H, Cortot A, Bollart C, Zaridze D, Brennan P, Boffetta P, Brambilla E, Hainaut P: **Patterns of EGFR, HER2, TP53, and KRAS mutations of p14arf expression in non-small cell lung cancers in relation to smoking history.** *Cancer Res* 2007, **67**:5667–5672.
3. Soda M, Choi YL, Enomoto M, Takada S, Yamashita Y, Ishikawa S, Fujiwara S, Watanabe H, Kurashina K, Hatanaka H, Bando M, Ohno S, Ishikawa Y, Aburatani H, Niki T, Sohara Y, Sugiyama Y, Mano H: **Identification of the transforming EML4-ALK fusion gene in non-small-cell lung cancer.** *Nature* 2007, **448**:561–566.
4. Koivunen JP, Mermel C, Zejnullahu K, Murphy C, Lifshits E, Holmes AJ, Choi HG, Kim J, Chiang D, Thomas R, Lee J, Richards WG, Sugarbaker DJ, Ducko C, Lindeman N, Marcoux JP, Engelman JA, Gray NS, Lee C, Meyerson M, Jänne PA: **EML4-ALK fusion gene and efficacy of an ALK kinase inhibitor in lung cancer.** *Clin Cancer Res* 2008, **14**:4275–4283.
5. Takeuchi K, Choi YL, Soda M, Inamura K, Togashi Y, Hatano S, Enomoto M, Takada S, Yamashita Y, Satoh Y, Okumura S, Nakagawa K, Ishikawa Y, Mano H: **Multiplex reverse transcription-PCR screening for EML4-ALK fusion transcripts.** *Clin Cancer Res* 2008, **14**:6618–6624.
6. Takeuchi K, Choi YL, Soda M, Inamura K, Togashi Y, Hatano S, Inamura K, Takada S, Ueno T, Yamashita Y, Satoh Y, Okumura S, Nakagawa K, Ishikawa Y, Mano H: **KIF5B-ALK, a novel fusion oncokinase identified by an immunohistochemistry-based diagnostic system for ALK-positive lung cancer.** *Clin Cancer Res* 2009, **15**:3143–3149.
7. Inamura K, Takeuchi K, Togashi Y, Nomura K, Ninomiya H, Okui M, Satoh Y, Okumura S, Nakagawa K, Soda M, Choi YL, Niki T, Mano H, Ishikawa Y: **EML4-ALK fusion is linked to histological characteristics in a subset of lung cancers.** *J Thorac Oncol* 2008, **3**:13–17.
8. Inamura K, Takeuchi K, Togashi Y, Hatano S, Ninomiya H, Motoi N, Mun MY, Sakao Y, Okumura S, Nakagawa K, Soda M, Choi YL, Mano H, Ishikawa Y: **EML4-ALK lung cancers are characterized by rare other mutations, a TTF-1 cell lineage, an acinar histology, and young onset.** *Mod Pathol* 2009, **22**:508–515.
9. Yoshida A, Tsuta K, Nakamura H, Kohno T, Takahashi F, Asamura H, Sekine I, Fukayama M, Shibata T, Furuta K, Tsuda H: **Comprehensive histologic analysis of ALK-rearranged lung carcinomas.** *Am J Surg Pathol* 2011, **5**:1226–1234.
10. Shaw AT, Yeap BY, Solomon BJ, Riely GJ, Gainor J, Engelman JA, Shapiro GI, Costa DB, Ou SH, Butaney M, Salgia R, Maki RG, Varella-Garcia M, Doebele RC, Bang YJ, Kulig K, Selaru P, Tang Y, Wilner KD, Kwak EL, Clark JW, Iafrate AJ, Camidge DR: **Effect of crizotinib on overall survival in patients with advanced non-small-cell lung cancer harbouring ALK gene rearrangement: a retrospective analysis.** *Lancet Oncol* 2011, **12**:1004–1012.
11. Kwak EL, Bang YJ, Camidge DR, Shaw AT, Solomon B, Maki RG, Ou SH, Dezube BJ, Jänne PA, Costa DB, Varella-Garcia M, Kim WH, Lynch TJ, Fidias P, Stubbs H, Engelman JA, Sequist LV, Tan W, Gandhi L, Mino-Kenudson M, Wei GC, Shreeve SM, Ratain MJ, Settleman J, Christensen JG, Haber DA, Wilner K, Salgia R, Shapiro GI, Clark JW, *et al*: **Anaplastic lymphoma kinase inhibition in non-small-cell lung cancer.** *N Engl J Med* 2010, **363**:1693–1703.
12. Ou SH, Kwak EL, Siwak-Tapp C, Dy J, Bergethon K, Clark JW, Camidge DR, Solomon BJ, Maki RG, Bang YJ, Kim DW, Christensen J, Tan W, Wilner KD, Salgia R, Iafrate AJ: **Activity of crizotinib (PF02341066), a dual mesenchymal-epithelial transition (MET) and anaplastic lymphoma kinase (ALK) inhibitor, in a non-small cell lung cancer patient with de novo MET amplification.** *J Thorac Oncol* 2011, **6**:942–946.
13. Osada H, Takahashi T: **Genetic alterations of multiple tumor suppressors and oncogenes in the carcinogenesis and progression of lung cancer.** *Oncogene* 2002, **21**:7421–7434.
14. Järvinen AK, Autio R, Kilpinen S, Saarela M, Leivo I, Grénman R, Mäkitie AA, Monni O: **High-resolution copy number and gene expression microarray analyses of head and neck squamous cell carcinoma cell lines of tongue and larynx.** *Gene Chromosome Canc* 2008, **47**:500–509.
15. Lo KC, Stein LC, Panzarella JA, Cowell JK, Hawthorn L: **Identification of genes involved in squamous cell carcinoma of the lung using synchronized data from DNA copy number and transcript expression profiling analysis.** *Lung Cancer* 2008, **59**:315–331.
16. Takeuchi K, Soda M, Togashi Y, Suzuki R, Sakata S, Hatano S, Asaka R, Hamanaka W, Ninomiya H, Uehara H, Lim Choi Y, Satoh Y, Okumura S, Nakagawa K, Mano H, Ishikawa Y: **RET, ROS1, and ALK Fusions in Lung Cancer.** *Nat Med* 2012, **18**:378–381.
17. Inamura K, Togashi Y, Nomura K, Ninomiya H, Hiramatsu M, Satoh Y, Okumura S, Nakagawa K, Ishikawa Y: **let-7 microRNA expression is reduced in bronchioloalveolar carcinoma, a non-invasive carcinoma, and is not correlated with prognosis.** *Lung Cancer* 2007, **58**:392–396.